OCEANICS INC.

THEORETICAL STUDY OF THE MOTIONS OF AN AIRCRAFT CARRIER AT SEA

by

Paul Kaplan

and

Theodore P. Sargent

Prepared For:

Office of Naval Research
Department of the Navy
Washington, D. C. 20360

Report No. 65-22

January, 1965

Technical Industrial Park / Plainview, N.Y.

THEORETICAL STUDY OF THE MOTIONS OF AN AIRCRAFT CARRIER AT SEA

by

Paul Kaplan

and

Theodore P. Sargent

Prepared For:

Office of Naval Research
Department of the Navy
Washington, D. C. 20360

Under Contract No. Nonr-4186(00)

Report No. 65-22

January, 1965

OCEANICS

FOREWORD

This report is one of a series of reports produced under Office of Naval Research Contract No. Nonr-4186(00), concerned with "Hydrodynamic Effects Influencing Aircraft Carrier Landing Operations". Two reports have previously been issued on the subject of experimental model scale measurements of the flow disturbances in the air wake of an aircraft carrier. The present report, dealing with ship motions at sea, will be followed by a fourth report of this series which is concerned with time history prediction of ship motions.

ABSTRACT

A mathematical model is developed for representing the heave, pitch and roll motions of an aircraft carrier at sea. The data is in the form of transfer functions relative to the waves, which are determined for a range of forward speeds and headings considered appropriate to carrier operations during the landing phase. From this information, spectral responses representing the statistical characteristics of motions in certain specific sea states are then developed. The results are presented in a form that can be applied to computer simulation studies for various types of wave disturbances, such as storm conditions, swells, and combinations of such wave systems.

The motions of heave and pitch are emphasized in this study, since roll motions are sufficiently small so that they do not significantly influence the aircraft landing operation. Certain limited conclusions as to motion severity and methods for reducing ship motions are outlined, together with recommendations for specific applications and extensions of the theoretical results.

TABLE OF CONTENTS

NOMENCLATURE

Symbol	Description
$A^2(\omega_e)$	Spectral energy distribution of waves referred to moving axis system
A'_{ij}	Component of added mass tensor
$\bar{A}_z$	Ratio of wave amplitude to heave amplitude for vertical motion-induced wave
a	Amplitude of surface wave elevation
a_{ij}	Matrix element for vertical plane motions
B*	Local beam of ship section
|BM|	Vertical distance between center of buoyancy and metacenter
CB	Center of buoyancy
CG	Center of gravity
c	Propagation speed of surface wave
E_i	Total energy (integrated area) under spectral curve
|GM|	Vertical distance between CG and metacenter
g	Acceleration due to gravity
$\bar{h}$	Average half-draft
I_t	Total roll moment of inertia (about x-axis)
I_{y_o}	Pitch moment of inertia (about y-axis)
$J(\omega_e)$	Jacobian of frequency transformation

Symbol	Description
K	Roll moment, positive about the x-axis
|KB|	Vertical distance from keel to CB
|KG|	Vertical distance from keel to CG
L	Length of ship
M	Pitch moment, positive about the y-axis
m_o	Mass of ship
N'_{zz}	Local heave damping coefficient
N_ϕ	Roll damping coefficient
|OB|	Vertical distance from CB to waterline
|OG|	Vertical distance from waterline to CG
|OM|	Vertical distance from waterline to metacenter
$p = \dot{\phi}$	Roll angular velocity
$R^2(\omega)$	Spectral energy of waves referred to a fixed position
S	Cross-sectional area of ship
s	Laplace transform operator
$T_{i\eta}$	Response operator (amplitude and phase relative to wave)
T_z, T_θ, T_ϕ	Transfer functions for heave, pitch, and roll, respectively, for response to swell
V	Forward speed
v	Lateral body velocity (along y-axis)
v_o	Lateral wave orbital velocity
v_w	Wind speed

Symbol	Description
W	Ship displacement
w_o	Vertical wave orbital velocity
x, y, z	Orthogonal axis system; x-axis horizontal positive toward the bow; y-axis horizontal positive to port; z-axis vertical positive upward. Also used to represent translational ship motions of sway (y), and heave (z) relative to a state of rest
x_b, x_s	Bow and stern x-coordinates, respectively
Y, Z	Forces acting positively along the y and z-axes, respectively
$\overline{z}_b$	Local sectional vertical center of buoyancy position
β	Heading angle of waves relative to ship heading
β_w	Heading angle of an individual wave relative to the wind
∇	Displaced volume
ζ_s	Damping factor for swell spectrum
η	Elevation of free surface
θ	Pitch angle, positive for rotation about y-axis
λ	Wavelength
ρ	Fluid mass density
$\Phi_i(\omega_e)$	Energy spectrum of particular motion
ϕ	Roll angle, positive about the x-axis
ϕ_z, ϕ_θ	Phase angles of heave and pitch, respectively, with regard to wave reference

Symbol	Description
ω	Circular frequency (rad./sec)
ω_e	Circular frequency of encounter
ω_s	Center frequency of swell

Subscripts (unless otherwise defined)

bm	Due to body motions (inertial effects)
d	Due to damping
h	Due to hydrostatic effects
o	Relative to waterline reference position
w	Due to waves

THEORETICAL STUDY OF THE MOTIONS OF AN AIRCRAFT CARRIER AT SEA

INTRODUCTION

The modern aircraft carrier essentially functions as a floating, mobile airfield at sea. However, this mobility, which is of prime importance for military tactics, has certain drawbacks of an operational nature during the aircraft landing phase due to specific inherent technical factors. While at sea, the carrier must achieve a proper heading (relative to the prevailing wind) and also a specific forward speed, so that a certain minimum wind-over-deck air velocity is maintained along the ...anted flight deck. There is then a continuous translatory motion of the landing deck as the aircraft is approaching for a landing. In addition, the carrier operates in the open sea, where the effects of waves result in continuous irregular oscillations of the ship in all six degrees of freedom. The varying deck displacements due to these ship motions are significant disturbances that affect the pilot's capability in carrying out a safe landing.

In order to aid the pilot in the landing operation, certain signal systems are used to provide a terminal guidance reference. A particular type of system presently used on U. S. Navy carriers is the Fresnel Lens Optical Landing System (FLOLS), which makes use of an optical image as an indicator (to the pilot) of proper glide path (a description of the FLOLS and its operating characteristics may be obtained, for example, from References [1] and [2]).

Since the actual lens system is located on the ship, and thereby partakes of the ship motions, the beam and the image of the FLOLS are affected by these motions, and hence the lens must be stabilized against these motions.

On the basis of the important influence of ship motions on the landing process, as outlined above, a theoretical study of the motion characteristics of aircraft carriers in waves was carried out and is reported herein. The information obtained in this program is in a form suitable for use in simulation studies, as a representation of an important environmental disturbance, which was the main intent of the study. In addition, knowledge of the ship motion characteristics is necessary for determining the required lens stabilization control rule; it supplies a base reference for determining the effects of possible ship motion stabilization methods, such as use of anti-pitch fins, anti-roll stabilizers, etc.; and it also provides the basic tools necessary for development of a motion (i. e. time history) prediction technique.

This work was carried out at OCEANICS, Inc. under the sponsorship of Air Programs, Office of Naval Research, Department of the Navy, under Contract number Nonr-4186(00).

ASSUMPTIONS AND TECHNIQUES USED IN ANALYSIS

The equations of motion used in this study will be formulated according to linear theory, thereby allowing a separation between the longitudinal modes of motion (in the vertical plane) and the lateral (horizontal plane) motions. As a further simplification, only the motions of the carrier that will affect the aircraft in its longitudinal motions will be considered. Thus heave, pitch and roll motions of the carrier will be studied (roll motion is included since it influences the vertical displacement of the landing deck and also the FLOLS lens unit). Heave and pitch motions will be coupled, and surge effects will be neglected due to their expected small influence for the present problem. The roll motion will be assumed to be coupled with sway motion, and effects of yaw will be neglected. This is based on an assumed small yaw influence, as well as the fact that yawing is appreciably influenced by the helmsman's input to the ship rudder, which is an extraneous influence not directly ascribed to an environmental (i. e. due to wave forces) input. Only uncontrolled ship motions, in direct response to wave effects, are considered in this study.

The equations of motion in regular waves are formulated according to linear theory by the balance of inertial, damping, restoring, exciting, and coupling forces and moments. Both hydrodynamic and hydrostatic effects due to the body-fluid interaction are included in the analysis. The hydrodynamic forces and moments such as damping, exciting effects due to waves, etc. will be

determined by application and/or extension of the methods described in [3] and [4], which are representative of a technique known as strip-theory (also referred to as a form of slender-body theory). This method makes the assumption that, for an elongated body with transverse dimensions small compared to its length, the flow at any cross-section is independent of the flow at any other section, and hence the flow problem is reduced to a two-dimensional problem in the transverse plane. The forces at each section are found by this method, and the total force is found by integrating over the body length.

Solutions will be obtained for regular sinusoidal seas with different wavelengths and headings relative to the ship, for different ship speeds. The actual conditions considered will be forward speeds of 10 knots, 20 knots, and 30 knots; wavelengths extending from half the ship length up to 2.5 times the ship length; and headings ranging from pure head seas to seas 45° off the bow. These conditions are considered sufficient to cover most of the practical operational situations associated with carrier landings. Response amplitude operators (i.e. transfer function amplitudes relative to the wave amplitude) are found from these solutions, together with the phases of the motions relative to the regular wave system.

The results for regular sinusoidal waves can be generalized to yield information on the motions in an irregular (random) seaway in terms of power spectra, which represent the relative amplitudes as a function of frequency. These motion power spectra can be operated upon to obtain information on

average values, probabilities of relatively high amplitudes of oscillation, etc. in the ship motion time histories, according to the methods of [5]. The oncoming irregular sea conditions are represented by a surface elevation (wave) spectrum as the input data for this process. Three different fully developed sea states were considered in this study, viz. Sea States 4, 5 and 6, where the spectral data for the different sea states were determined from [6]. Similarly, spectral response data were obtained for various swell conditions (i.e. irregular waves of varying amplitude, but with almost constant period) by developing narrow band filters for wave representations, in conjunction with the regular wave response operators. The particular techniques, results, etc. developed for this purpose will be discussed in detail in a later section of this report.

The particular aircraft carrier class studied in detail in this program was the U.S.S. Forrestal (CVA-59) class, which is representative of a number of large attack carriers. Some initial consideration was given to the evaluation of motion characteristics of the U.S.S. Midway class as well, but up-to-date information on the present body lines, configurations, etc. of that ship was not readily available [7]. Therefore only some indications of how to make use of the Forrestal-class data to determine approximate motion characteristics of Midway-class carriers will be given in a later section of this report. A summary of the numerical values of the important parameters characterizing the U.S.S. Forrestal, for which computations in the present study were carried out, is

presented in Table 1. Body lines, section characteristics, etc. were determined from [8].

TABLE 1

NUMERICAL VALUES OF U. S. S. FORRESTAL SHIP CHARACTERISTICS

Length(LBP), ft.	990
Beam, ft.	129.33
Draft, ft.	35.8
Displacement, tons	78,037
Metacentric height, $\|GM\|$, ft.	12.5
Vertical distance from keel to CG, $\|KG\|$, ft.	44.6
Vertical distance from keel to CB, $\|KB\|$, ft.	19.65
Pitch moment of inertia, without added fluid inertia[1], slug-ft.^{2}	335.97×10^9
Total roll moment of inertia (including added fluid inertia)[2], slug-ft.^{2}	21.97×10^9
Heave period[3], sec.	8.69
Pitch period[3], sec.	9.10
Roll period[3], sec.	19.82

1. Assuming longitudinal gyradius = 0.25 L.
2. Obtained from knowledge of natural roll period, displacement, and metacentric height.
3. Obtained from David Taylor Model Basin letter [9] and subsequent discussions with DTMB personnel. All conditions outlined in Table 1 above were selected to conform to conditions of model tests carried out at DTMB.

EQUATIONS OF MOTION

The equations of motion are formulated relative to an axis system whose origin is located at the CG of the ship. A right-handed cartesian coordinate system is selected with the axes fixed in the body, with the x-axis positive toward the bow (in the direction of forward motion), the y-axis positive to port, and the z-axis positive upward. These axes are defined to have a fixed orientation, i.e. they do not rotate with the body, but they can translate with the body. The ship angular motions can be considered to be small oscillations about a mean position given by the axes. The dynamic variables in this study are the displacements y and z along the respective axes, and the angular displacements ϕ (roll) and θ (pitch) which are defined as positive in the direction of positive rotation about the x and y-axes, respectively. (It should be noted that the present axis system differs from that used by Korvin-Kroukovsky and Jacobs[3] in regard to the positive direction of pitch angle θ. Results and equations in the present study can be related to those in [3] by changing the sign of θ, positive pitch moment, etc. in order to obtain data for pitch angle that is considered positive bow-up, the usual naval reference condition).

The hydrodynamic forces and moments are composed of terms of inertial nature due to body dynamic motions; dissipative terms due to damping action; and exciting effects due to the oncoming waves. The effect of the free surface is accounted for in the inertial and wave forces by frequency dependent factors that modify the added masses, and all couplings of inertial and dissipative nature are

included in the analysis. For the dynamic body motions, the slender body theory result in terms of fluid momentum [4] will yield a local sectional vertical force given by

$$\frac{dZ_{bm}}{dx} = - A'_{33}(\ddot{z} - x\ddot{\theta} + 2V\dot{\theta}) + V(\dot{z} - x\dot{\theta} + V\theta) \frac{dA'_{33}}{dx} \tag{1}$$

where Z_{bm} is the vertical force due to dynamic body motions; A'_{33} is the sectional vertical added mass; z is heave displacement; θ is the pitch angle; and V is the forward speed. Integration of this result over the ship hull, with the assumption that $A'_{33}(x_b) = A'_{33}(x_s) = 0$, i. e. at the bow and stern extremities, results in

$$Z_{bm} = - \int_{x_s}^{x_b} A'_{33} dx \cdot \ddot{z} + \int_{x_s}^{x_b} A'_{33}\, x dx \cdot \ddot{\theta} - V \int_{x_s}^{x_b} A'_{33}\, dx \cdot \dot{\theta} \tag{2}$$

The data for determining the value of A'_{33} was obtained from the work of Grim [10], with A'_{33} defined by

$$A'_{33} = C \frac{\rho \pi B^{*2}}{8} \tag{3}$$

where B* is the local section beam and the coefficient C is represented graphically as a function of a dimensionless frequency parameter and two sectional geometric parameters (beam-draft ratio and section coefficient).

The damping force in heave arises due to energy dissipation associated with wave generation by the ship motions on the free surface. The ratio of the amplitude of the heave-generated two-dimensional waves to the heave motion amplitude of a section is denoted as $\bar{A}_z$, and by equating the energy balance

between ship work and outgoing wave energy, the vertical damping force per unit vertical velocity of the section is expressed as

$$N'_{zz} = \frac{\rho g^2 \bar{A}_z^2}{\omega_e^3} \tag{4}$$

where ω_e is the frequency of oscillation. Values of $\bar{A}_z$ were obtained from the work of Grim [10] as functions of the same parameters as for A'_{33}, using appropriate interpolation of the graphs to obtain the required values. The vertical damping force at each section is then

$$\frac{dZ_d}{dx} = - N'_{zz}(\dot{z} - x\dot{\theta} + V\theta) \quad , \tag{5}$$

and the total vertical damping force is determined by integrating over the ship length, leading to

$$Z_d = - \int_{x_s}^{x_b} N'_{zz} dx \cdot \dot{z} + \int_{x_s}^{x_b} N'_{zz} x dx \cdot \dot{\theta} - V \int_{x_s}^{x_b} N'_{zz} dx \cdot \theta \quad , \tag{6}$$

The wave exciting force is obtained by a combination of terms due to inertial effects (via slender-body theory) and the predominant hydrostatic effect that arises due to periodic buoyancy alterations as the (sinusoidal) waves progress past the ship hull. The hydrostatic restoring force due to static vertical displacement (on a calm free surface) of a ship section is

$$\frac{dZ_h}{dx} = - \rho g B(z - x\theta) \quad , \tag{7}$$

leading to a total force given by

$$Z_h = -\rho g \int_{x_s}^{x_b} B^* dx \cdot z + \rho g \int_{x_s}^{x_b} B^* x dx \cdot \theta \qquad (8)$$

In a similar manner, the buoyancy term in the wave force is given, for a local ship section, as

$$\frac{dZ_w^{(1)}}{dx} = \rho g B^* \eta(x,t) \qquad (9)$$

where $\eta(x,t)$ is the wave elevation. The waves are assumed to be propagating in a direction defined by the angle β, where β is the angle between the x-axis and the normal to the wave crests, which lies in the range $-\frac{\pi}{2} \leq \beta \leq \frac{\pi}{2}$. The wave propagation speed c is taken to be < 0 for head seas, i.e. $c = -|c|$, and the expression for $\eta(x,t)$ in terms of the moving (i.e. translating in the x-direction) axis system is

$$\eta(x,t) = a \sin\left[\frac{2\pi x}{\lambda} \cos\beta + \omega_e t\right] \qquad (10)$$

where

$$\omega_e = \frac{2\pi}{\lambda}(V\cos\beta + |c|) \qquad (11)$$

$$|c| = \sqrt{\frac{g\lambda}{2\pi}} \qquad (12)$$

and the wave elevation is evaluated along the ship centerline, i.e. $y = 0$, in accordance with linear theory. The total hydrostatic wave force is then

$$Z_w^{(1)} = \rho g a \left\{ \cos\omega_e t \int_{x_s}^{x_b} B^* \sin\left(\frac{2\pi x}{\lambda}\cos\beta\right) dx + \sin\omega_e t \int_{x_s}^{x_b} B^* \cos\left(\frac{2\pi x}{\lambda}\cos\beta\right) dx \right\} \qquad (13)$$

The hydrodynamic part of the wave force is assumed to be primarily due to inertial effects only, and is obtained by application of slender-body theory [4], [11] carried over to the surface ship case. The local force may be represented by

$$\frac{dZ_w^{(2)}}{dx} = \rho S \frac{Dw_o}{Dt} + \frac{D}{Dt}(A'_{33} w_o) \tag{14}$$

where S is cross-sectional area, the operator $\frac{D}{Dt}$ is

$$\frac{D}{Dt} = \frac{\partial}{\partial t} - V \frac{\partial}{\partial x} \tag{15}$$

and w_o is the vertical orbital velocity (at the depth of the CB), given by

$$w_o = -\frac{2\pi a|c|}{\lambda} e^{-2\pi \bar{h}/\lambda} \cos\left[\frac{2\pi x}{\lambda}\cos\beta + \omega_e t\right] \tag{16}$$

The CB depth, denoted as $\bar{h}$ in Equation (16), is included here as an approximate allowance for the exponential decay of waves. The final expression for the hydrodynamic wave force, obtained by evaluating Equation (14) and integrating over the ship length, is given by

$$\begin{aligned} Z_w^{(2)} = -\frac{2\pi a g}{\lambda} e^{-2\pi \bar{h}/\lambda} \Bigg\{ & \cos\omega_e t \left[\int_{x_s}^{x_b} (\rho S + A'_{33}) \sin\left(\frac{2\pi x}{\lambda}\cos\beta\right) dx \right. \\ & \left. + \frac{V}{|c|}\cos\beta \int_{x_s}^{x_b} A'_{33} \sin\left(\frac{2\pi x}{\lambda}\cos\beta\right) dx \right] \\ & + \sin\omega_e t \left[\int_{x_s}^{x_b} (\rho S + A'_{33}) \cos\left(\frac{2\pi x}{\lambda}\cos\beta\right) dx \right. \\ & \left. + \frac{V}{|c|}\cos\beta \int_{x_s}^{x_b} A'_{33} \cos\left(\frac{2\pi x}{\lambda}\cos\beta\right) dx \right] \Bigg\} , \end{aligned} \tag{17}$$

and the total wave excitation force is then

$$Z_w = Z_w^{(1)} + Z_w^{(2)} \tag{18}$$

The pitch moment terms corresponding to all the force terms derived in the foregoing are easily obtained by use of the relation

$$\frac{dM}{dx} = -x\frac{dZ}{dx} \quad , \tag{19}$$

followed by the required integrations over the hull. This leads to

$$M_{bm} = \int_{x_s}^{x_b} A'_{33}\, x dx \cdot \ddot{z} - \int_{x_s}^{x_b} A'_{33} x^2\, dx \cdot \ddot{\theta} + V \int_{x_s}^{x_b} A'_{33} dx \cdot \dot{z}$$

$$+ V^2 \int_{x_s}^{x_b} A'_{33} dx \cdot \theta \, , \tag{20}$$

$$M_d = \int_{x_s}^{x_b} N'_{zz}\, x dx \cdot \dot{z} - \int_{x_s}^{x_b} N'_{zz}\, x^2 dx \cdot \dot{\theta} + V \int_{x_s}^{x_b} N'_{zz}\, x dx \cdot \theta \, , \tag{21}$$

$$M_h = \rho g \int_{x_s}^{x_b} B^* x dx \cdot z - \rho g \int_{x_s}^{x_b} B^* x^2 dx \cdot \theta \, , \tag{22}$$

$$M_w^{(1)} = -\rho g a \left\{ \cos \omega_e t \int_{x_s}^{x_b} x B^* \sin\left(\frac{2\pi x}{\lambda} \cos\beta\right) dx \right.$$

$$\left. + \sin \omega_e t \int_{x_s}^{x_b} x B^* \cos\left(\frac{2\pi x}{\lambda} \cos\beta\right) dx \right\} \tag{23}$$

$$M_w^{(2)} = \frac{2\pi a g}{\lambda} e^{-2\pi\bar{h}/\lambda}\Bigg\{\cos\omega_e t\Bigg[\int_{x_s}^{x_b} x(\rho S+A'_{33})\sin\left(\frac{2\pi x}{\lambda}\cos\beta\right)dx + \frac{V}{|c|}\cos\beta\int_{x_s}^{x_b} xA'_{33}\sin\left(\frac{2\pi x}{\lambda}\cos\beta\right)dx - \frac{V\lambda}{2\pi|c|}\int_{x_s}^{x_b} A'_{33}\cos\left(\frac{2\pi x}{\lambda}\cos\beta\right)dx\Bigg] + \sin\omega_e t\Bigg[\int_{x_s}^{x_b} x(\rho S+A'_{33})\cos\left(\frac{2\pi x}{\lambda}\cos\beta\right)dx + \frac{V}{|c|}\cos\beta\int_{x_s}^{x_b} x\,A'_{33}\cos\left(\frac{2\pi x}{\lambda}\cos\beta\right)dx + \frac{V\lambda}{2\pi|c|}\int_{x_s}^{x_b} A'_{33}\sin\left(\frac{2\pi x}{\lambda}\cos\beta\right)dx\Bigg]\Bigg\} \quad (24)$$

The equations of motion are given by

$$m_o\ddot{z} = Z_{bm} + Z_d + Z_h + Z_w \quad (25)$$

$$I_{y_o}\ddot{\theta} = M_{bm} + M_d + M_h + M_w \quad (26)$$

where m_o = mass of ship, I_{y_o} = moment of inertia of ship about the y-axis; they may be written in the simplified form

$$a_{11}\ddot{z} + a_{12}\dot{z} + a_{13}z + a_{14}\ddot{\theta} + a_{15}\dot{\theta} + a_{16}\theta = Z_w \tag{27}$$

$$a_{21}\ddot{z} + a_{22}\dot{z} + a_{23}z + a_{24}\ddot{\theta} + a_{25}\dot{\theta} + a_{26}\theta = M_w , \tag{28}$$

where

$$\left.\begin{aligned}
&a_{11} = m_o + \int_{x_s}^{x_b} A'_{33}\,dx;\ a_{12} = \int_{x_s}^{x_b} N'_{zz}\,dx;\ a_{13} = \rho g \int_{x_s}^{x_b} B^*\,dx;\\
&a_{14} = -\int_{x_s}^{x_b} A'_{33}\,x\,dx;\ a_{15} = V\int_{x_s}^{x_b} A'_{33}\,dx - \int_{x_s}^{x_b} N'_{zz}\,x\,dx;\\
&a_{16} = V\int_{x_s}^{x_b} N'_{zz}\,dx - \rho g \int_{x_s}^{x_b} B^*\,x\,dx;\ a_{21} = -\int_{x_s}^{x_b} A'_{33}\,x\,dx;\\
&a_{22} = -\int_{x_s}^{x_b} N'_{zz}\,x\,dx - V\int_{x_s}^{x_b} A'_{33}\,dx;\ a_{23} = -\rho g \int_{x_s}^{x_b} B^*\,x\,dx;\\
&a_{24} = I_{y_o} + \int_{x_s}^{x_b} A'_{33}\,x^2\,dx;\ a_{25} = \int_{x_s}^{x_b} N'_{zz}\,x^2\,dx;\\
&a_{26} = \rho g \int_{x_s}^{x_b} B^*x^2\,dx - V\int_{x_s}^{x_b} N'_{zz}\,x\,dx - V^2\int_{x_s}^{x_b} A'_{33}\,dx
\end{aligned}\right\} \tag{29}$$

The wave force and moment are separated into the forms

$$Z_w = Z_{wc} \cos \omega_e t + Z_{ws} \sin \omega_e t \tag{30}$$

$$M_w + M_{wc} \cos \omega_e t + M_{ws} \sin \omega_e t \tag{31}$$

and this allows simple computational procedures for determining solutions of the ship heave and pitch response characteristics (i. e. amplitude and phase) relative to the oncoming sinusoidal waves.

The roll motion is found by solving the coupled roll-sway equations, on the assumption that yawing motion per se has small influence on roll. In these two degrees of freedom, the application of slender-body theory to a ship section can be shown to lead to an expression for the inertial sway force given by

$$\frac{dY_{bm}}{dx} = - \frac{D}{Dt} (A'_{22} v) - \frac{D}{Dt} (A'_{42} p) \ , \tag{32}$$

with v the sway velocity and $p = \dot{\phi}$ the roll angular velocity. Integration over the hull, with the assumption that the generalized inertia terms A'_{22} and A'_{42} vanish at the ends, leads to

$$Y_{bm} = - A_{22} \dot{v} - A_{42} \dot{p} \tag{33}$$

where

$$A_{22} = \int_{x_s}^{x_b} A'_{22} dx \ , \quad A_{42} = \int_{x_s}^{x_b} A'_{42} \, dx \tag{34}$$

In the development of the sway motion equation, since there is no restoring force and the major effect is inertial, damping in sway and any frequency dependence in the inertial terms A'_{22} and A'_{42} will be neglected (the zero frequency limits are used). The lateral wave exciting force (neglecting the effect of the factor $e^{-2\pi\bar{h}/\lambda}$) is given by

$$\frac{dY_w}{dx} = \rho S \frac{Dv_o}{Dt} + \frac{D}{Dt}(A'_{22} v_o) \tag{35}$$

where

$$v_o = -\frac{2\pi a|c|}{\lambda} \sin\beta \sin\left(\frac{2\pi x}{\lambda}\cos\beta + \omega_e t\right) , \tag{36}$$

which leads to

$$Y_w = -\frac{2\pi a g}{\lambda} \sin\beta \int_{x_s}^{x_b} \left[\rho S + A'_{22}\left(1 - \frac{V}{|c|}\cos\beta\right)\right] \cos\left(\frac{2\pi x}{\lambda}\cos\beta + \omega_e t\right) dx \tag{37}$$

The sway equation of motion is then given by

$$(m_o + A_{22})\dot{v} + A_{42}\ddot{\phi} = Y_w , \tag{38}$$

and it remains to derive the roll equation of motion in order to solve the coupled system.

The roll equation is derived on the basis of certain simplifying assumptions. The inertial roll moment due to body dynamic motions is expressed as

$$K_{bm} = -A_{42}\dot{v} - A_{44}\ddot{\phi} \tag{39}$$

where A_{44} is the total added roll moment of inertia due to the fluid. The hydrostatic restoring force in roll is a classical result of naval architecture, and is expressed here as

$$K_h = - \rho g \nabla |GM| \phi = - W |GM| \phi \qquad (40)$$

where ∇ is the displaced volume, $|GM|$ is the metacentric height (distance between the CG and the metacenter M), and $W = \rho g \nabla$ is the ship displacement. The roll damping moment is represented in the form

$$K_d = - N_\phi \dot{\phi} \quad , \qquad (41)$$

where the value of the coefficient N_ϕ is a constant determined from available experimental data on the damping ratio obtained in a roll-decay model experiment [9]. It is assumed that the major influence on roll is due to the pure roll damping term, and other motion damping terms are neglected. Furthermore, since roll is a lightly damped motion, the value of damping is only important near resonance, and the constant value obtained in the roll decay tests is valid for this purpose.

The hydrodynamic added masses A_{22} and A_{42} required in the roll analysis are obtained by integrating the sectional values (A'_{22} and A'_{42}) over the hull, where these sectional values are obtained from information in [12]. Particular care is necessary, however, in the determination of A'_{42}, which is a term referenced to the CG position, while the values in [12] are appropriate to a reference at the waterline. Denoting the waterline location as 0, and with the CG of the ship located above the waterline, the roll moment about the CG (as

used in this study) is

$$K = K_o + |OG|\ Y \quad , \tag{42}$$

where OG is the distance from the waterline to the ship CG. For the contribution due to sway acceleration $\dot{v}$,

$$\begin{aligned} K &= -A_{42_o}\dot{v} + |OG|\ (-A_{22}\dot{v}) \\ &= -(A_{42_o} + |OG|\ A_{22})\,\dot{v} \\ &= -A_{42}\dot{v} \quad , \end{aligned} \tag{43}$$

with the local value A'_{42} interpreted as

$$A'_{42} = A'_{42_o} + |OG|\ A'_{22}. \tag{44}$$

The value of A_{44}, the added roll moment of inertia, is not found directly but is included with the body roll moment of inertia in the total effective roll moment of inertia. The value of that quantity is determined from experimental knowledge of the roll natural period, metacentric height, etc. which are supplied by [9].

The roll moment due to waves is determined by use of the relation in Equation (42), viz.

$$K_w = K_{w_o} + |OG|\ Y_w \tag{45}$$

where Y_w is given by Equation (37) and K_{w_o} is the roll moment given in [12]. This term is given by

$$\frac{dK_{w_o}}{dx} = \frac{D}{Dt}(A'_{42_o} v_o) - \rho\left[S\bar{z}_b + \frac{2}{3}\left(\frac{B^*}{2}\right)^3\right] \frac{Dv_o}{Dt} \tag{46}$$

where v_o is given by Equation (36), $\bar{z}_b$ is the local section vertical center of buoyancy position which is a negative quantity in the present case), and where additional terms involving the local body potential have been neglected for simplicity and in expectation of their small contribution to the total wave induced roll moment. The term on the right in Equation (46) will result in terms requiring integration over the huli, with sinusoidal weighting functions dependent on the wavelength, but it has been found that for the present case the result will not be significantly in error if the term in brackets is replaced by simple geometric constants of the ship, so that the approximations

$$\int_{x_s}^{x_b} S\bar{z}_b \frac{Dv_o}{Dt}\, dx \simeq -|OB| \int_{x_s}^{x_b} S \frac{Dv_o}{Dt}\, dx \tag{47}$$

$$\int_{x_s}^{x_b} \frac{2}{3}\left(\frac{B^*}{2}\right)^3 \frac{Dv_o}{Dt}\, dx \simeq |BM| \int_{x_s}^{x_b} S \frac{Dv_o}{Dt}\, dx \tag{48}$$

are valid in this case, where $|OB|$ is the distance from the waterline to the CB and $|BM|$ is the metacentric radius (distance from CB to metacenter M). This approximation results in

$$\frac{dK_{w_o}}{dx} = \frac{D}{Dt}(A'_{42_o} v_o) - \rho |OM| S \frac{Dv_o}{Dt}\ , \tag{49}$$

where |OM| is the distance from the waterline to the metacenter, and in accordance with Equation (45) leads to the roll moment due to waves given by

$$K_w = \frac{2\pi a}{\lambda}\rho g \sin\beta\,|GM| \int_{x_s}^{x_b} S \cos\left(\frac{2\pi x}{\lambda}\cos\beta + \omega_e t\right) dx$$

$$- \frac{2\pi a}{\lambda} g \sin\beta\left(1 - \frac{V}{|c|}\cos\beta\right) \int_{x_s}^{x_b} A'_{42} \cos\left(\frac{2\pi x}{\lambda}\cos\beta + \omega_e t\right) dx \qquad (50)$$

The roll equation of motion is then

$$I_t\ddot{\phi} + N_\phi\dot{\phi} + W|GM|\phi + A_{42}\dot{v} = K_w\,, \qquad (51)$$

where I_t is the total effective roll moment of inertia (including added fluid inertia), and after eliminating v by use of Equation (38) the equation in terms of pure rolling motion alone is

$$\left(I_t - \frac{A_{42}^2}{m_o + A_{22}}\right)\ddot{\phi} + N_\phi\dot{\phi} + W|GM|\phi =$$

$$\frac{2\pi a}{\lambda}\rho g \sin\beta\,|GM| \int_{x_s}^{x_b} S \cos\left(\frac{2\pi x}{\lambda}\cos\beta + \omega_e t\right) dx$$

$$+ \frac{2\pi a}{\lambda} g \sin\beta\left\{\frac{A_{42}}{m_o + A_{22}} \int_{x_s}^{x_b}\left[\rho S + A'_{22}\left(1 - \frac{V}{|c|}\cos\beta\right)\right]\cos\left(\frac{2\pi x}{\lambda}\cos\beta + \omega_e t\right) dx\right.$$

$$\left. -\left(1 - \frac{V}{|c|}\cos\beta\right) \int_{x_s}^{x_b} A'_{42}\cos\left(\frac{2\pi x}{\lambda}\cos\beta + \omega_e t\right) dx\right. \qquad (52)$$

SOLUTION OF EQUATIONS OF MOTION

The coupled heave and pitch motions given by Equations (27) - (31) are solved by representing the responses in the form

$$z = z_1 \cos \omega_e t + z_2 \sin \omega_e t \tag{53}$$

and

$$\theta = \theta_1 \cos \omega_e t + \theta_2 \sin \omega_e t \tag{54}$$

The response relative to a unit wave height is found in the form of an amplitude and phase relative to the wave at the center of gravity (the equation reference position) in the following way:

$$\left| \frac{z}{a} \right| = \frac{\sqrt{z_1^2 + z_2^2}}{a} \quad , \quad \phi_z = \tan^{-1} \frac{z_1}{z_2} \tag{55}$$

and

$$\left| \frac{\theta}{a} \right| = \frac{\sqrt{\theta_1^2 + \theta_2^2}}{a} \quad , \quad \phi_\theta = \tan^{-1} \frac{\theta_1}{\theta_2} \tag{56}$$

The coefficients of the heave and pitch equations, given in Equation (29), are functionally dependent upon the frequency of encounter ω_e, and hence the system of equations is then a linear set of differential equations with frequency dependent coefficients. Solution of these equations, even with a computer, is complicated due to the necessity of evaluating the coefficients for each particular frequency considered, independent of the fact that the excitation is also dependent upon the frequency. This situation does not allow a simple interpretation of the basic

dynamics of the ship system in these modes of motion, since a single characteristic equation does not result. During the course of discussions concerning the use of the results in a simulation study of landing operations aboard aircraft carriers at sea, it was suggested[13] that the equations be reformulated with the use of constant coefficients in order to result in a single characteristic equation that determines the basic ship dynamics for a particular forward speed. This suggestion is based upon the fact that aircraft stability and control techniques make use of constant coefficient equations (e. g. see [14]) even though there is often frequency dependence exhibited in the stability derivatives obtained from model tests. As a result this approach was carried out by selecting certain constant values of the various coefficients in the equations of motion, with these constants selected in such a way that the basic dynamic characteristics of the system will be exhibited. Since information on the natural periods and the damping ratios for heave and pitch were available (see Table 1 and [9]), values of the added mass, heave damping, added pitch moment of inertia, and pitch damping were selected in order to exhibit some agreement with model data. Typical examples of values selected for the constant coefficient approach, shown relative to the actual variation of the quality as a function of frequency, are shown in Figures 1 and 2. The final coefficients occurring in the heave and pitch equations of motion are given in tabular form below in Table 2 for the various speeds of interest.

TABLE 2

Numerical Values of Coefficients in Heave and Pitch Equations

V =	0	10 kts.	20 kts.	30 kts.
a_{11}	$.121 \times 10^{8}$			
a_{12}	$.376 \times 10^{7}$			
a_{13}	$.615 \times 10^{7}$			
a_{14}	$.407 \times 10^{9}$			
a_{15}	$.245 \times 10^{9}$	$.357 \times 10^{9}$	$.469 \times 10^{9}$	$.581 \times 10^{9}$
a_{16}	$.252 \times 10^{9}$	$.316 \times 10^{9}$	$.379 \times 10^{9}$	$.443 \times 10^{9}$
a_{21}	$.407 \times 10^{9}$			
a_{22}	$.245 \times 10^{9}$	$.133 \times 10^{9}$	$.206 \times 10^{8}$	$-.915 \times 10^{8}$
a_{23}	$.252 \times 10^{9}$			
a_{24}	$.658 \times 10^{12}$			
a_{25}	$.218 \times 10^{12}$			
a_{26}	$.348 \times 10^{12}$	$.350 \times 10^{12}$	$.349 \times 10^{12}$	$.343 \times 10^{12}$

(The lines across the page indicate a constant value for all forward speeds, V)

A comparison of the full scale values of the heave and pitch natural periods and damping ratios, obtained at zero speed from the constant coefficient equations, with those obtained from model experiment (scaled to full scale values) is shown below in Table 3.

TABLE 3

Comparison of Theoretical and Experimental Natural Periods and Damping Ratios

Motion	Natural Period		Damping Ratio	
	Theory	Experiment	Theory	Experiment
Heave	8.80 sec.	8.69 sec.	.22	.26
Pitch	8.65 sec.	9.10 sec.	.23	.20

In view of the fairly good agreement shown for the conditions near resonance, it is then necessary to carry out more detailed computations over a complete frequency range in order to see if this approach with constant coefficients would yield useful results.

An example of results computed using the frequency dependent coefficients is shown in Figures 3 and 4 (amplitude ratios) for the particular case of 20 knot forward speed. Similar close agreement is shown for the case of phase angles. It can be seen that there is fairly close agreement such that the simpler approach with constant coefficients can be used throughout the entire range of conditions required in this program.

The results of the computations of amplitude response and phase angle, for the forward speeds of 10 knots, 20 knots, and 30 knots, and for headings relative to the bow (head seas) ranging from 0^{o} to 45^{o} (in 15^{o} increments) are shown in Figures 5 through 10. It can be seen that the results in regard to amplitude and phase, when plotted as functions of the frequency of encounter ω_e are quite close for the different headings, in spite of the fact that it is known that the responses for the same wavelength and forward speed will differ for the various headings. While there is no exact agreement, the results are sufficiently close over most of the frequency range where significant responses occur, with

the major deviation occurring at the higher frequencies where the motions are quite small. This is an interesting result, which may possibly be due to the fac that the ship is very long and the wavelengths necessary for appreciable motion (approximately $\frac{3}{4}$L and longer) will result in approximately equivalent wave forces, even though the wavelengths differ for the different headings at the same forward speed. Checking some of these relationships indicated that such a result would occur in a number of instances, and it is possible that that is the reason for the "collapsed" appearance of the response plots. While no definite substantiating experimental data was obtained in detail, some preliminary checking with results obtained in the course of tests at David Taylor Model Basin has shown fair agreemert with these conclusions for the cases that were checked. However, it will certainly be necessary to obtain further verification of these results in detail with the complete results of those experiments when they are published.

The results obtained in the present study are still useful, since the intent of the study was to provide data for simulation purposes so that environmental influences due to ship motion will be accounted for in the overall program. In the course of the checking with experimental data it was found that there was fairly good agreement in regard to the pitch motion characteristics, with the heave motion characteristics determined in this program underestimating the experimental values. The experimental information was obtained from the limited instances of examining the raw data obtained during the David Taylor Model Basin tests, and also from some regular wave tests carried out at the Massachusetts Institute of Technology Ship Model Towing Tank (for head seas) in the course of another aspect of this program [15]. The fact that the

pitch motion is represented fairly well, and the heave information does not have such good agreement, is typical of certain aspects of the strip theory approach used here (see [16] and [17] for a discussion of the limits of this theory).

Computations for roll motion were carried out using Equation (52), where the values of the roll damping coefficient N_ϕ was obtained using the information provided by [9] concerning the roll damping ratio. Computations of the roll amplitude were carried out, but the results indicated extremely small roll amplitudes for the frequency range considered in this program. The only perceptible response will occur in beam seas, and since the natural period of roll is so long, such responses will not be considered in detail since they do not correspond to useful operational conditions at sea. The details of the roll characteristics will be presented when considering the response characteristics in random seas, which will be treated in the next section.

STATISTICAL CHARACTERISTICS OF MOTIONS IN RANDOM SEAS

To characterize the motions of a ship in a random sea, where the motions themselves have a random nature, the function known as the energy spectrum of the motion must be found. This spectrum is a measure of the variation of the squares of the amplitudes of the various sinusoidal components of the motion, presented as a function of the frequency of encounter and the wave direction. For an arbitrary motion, represented by the i-subscript, the energy spectrum of that motion due to the effects of irregular random waves is represented by

$$\Phi_i(\omega_e) = \left|T_{i\eta}(\omega_e)\right|^2 A^2(\omega_e) \tag{57}$$

for a particular fixed ship heading in a unidirectional sea, where $A^2(\omega_e)$ is the wave spectrum and $\left|T_{i\eta}\right|$ is the response amplitude operator for that heading (amplitude of motion per unit wave amplitude). Since the response of the ship is determined as a function of the frequency of encounter ω_e, it is necessary to represent the wave spectrum also as a function of ω_e so that the total area under the spectrum (which is a necessary characteristic in determining statistical information on response characteristics) can be easily determined by integration with respect to ω_e. The wave spectrum used in this study is the Neumann form represented by

$$R^2(\omega) = C\omega^{-6} e^{-2g^2/(v_w\omega)^2} \tag{58}$$

where C is an empirical constant having the value 51.5 ft.^{2}/sec.^{5}, v_w is the wind speed in units of ft./sec., and the wave spectrum $R^2(\omega)$ has the units ft.^{2}-sec. The frequency ω appearing within the expression of the wave spectrum is the pure wave frequency, related to the wavelength λ by

$$\omega = \sqrt{\frac{2\pi g}{\lambda}} \tag{59}$$

The frequency of encounter ω_e can be shown to be related to ω by

$$\omega_e = \omega + \frac{\omega^2 V}{g} \cos\beta \quad , \tag{60}$$

and it is necessary when representing the wave spectrum as a function of ω_e to present it in the form given by

$$A^2(\omega_e) = R^2[\omega(\omega_e)]\, J(\omega_e) \tag{61}$$

where $J(\omega_e)$ is the Jacobian given by

$$J(\omega_e) = \frac{\partial\omega}{\partial\omega_e} = \frac{1}{\sqrt{1 + \frac{4\omega_e V}{g}\cos\beta}} \tag{62}$$

(see [5] for details). It is possible to represent the wave spectrum for a non-unidirectional sea, allowing for angular variation (a two-dimensional spectrum) which results in a modification to the basic Neumann formulation given by

$$R^2(\omega) = \begin{cases} \frac{2}{\pi} C\omega^{-6} e^{-2g^2/(v_w\omega)^2} \cos^2\beta_w, & -\frac{\pi}{2} < \beta_w < \frac{\pi}{2} \\ 0, \text{ otherwise} \end{cases} \tag{63}$$

where β_w is an angle measured from the direction toward which the wind is blowing (the predominant wave direction). In that case the motion spectrum that would occur for a particular ship heading measured relative to the wind direction can be obtained by integrating with respect to the angle β_w, but for simplicity in this particular study consideration has only been devoted to unidirectional seas. An illustration of the effective spectra, including the Jacobian term, is shown as a function of ω_e for Sea State 6 (defined by [6]) for two different headings of a ship relative to the unidirectional waves in Figures 17 and 18 for the various forward speeds considered in this study.

The spectral technique for analyzing random irregular time histories of motion, as embodied in the formulas given above, is applicable to linear systems only, since in that case a unique response amplitude operator is obtained. The spectral techniques used herein follow from linear superposition of the responses to individual frequency components contained in the excitation, and the final synthesis of the effects (in a mean-square sense) is represented by the motion spectrum.

From the spectral density function $\Phi_i(\omega_e)$ for a particular motion, there may be obtained, in principle, all the statistical or probabilistic properties possessed by the random process. For example, the total area E_i under the spectral-density function curve, as defined above,

$$E_i = \int_0^\infty \Phi_i(\omega_e)\, d\omega_e$$

is equal to $2\sigma_i^2$, i.e. twice the variance of the ordinates on the corresponding time-history curve. Here the ordinate dispersion, or standard deviation, has been denoted by σ_i, which is the root-mean-square value of the deviations of the ordinates from the mean or average ordinate which is assumed to be zero in this study.

Under the assumption that the seaway is a Gaussian or normal stochastic process which is exciting a linear system (in this case, the aircraft carrier), the responses of the system will in turn represent a Gaussian stochastic process. Characteristics of the motion time history may be obtained in terms of the quantity E_i by relating the behavior of the envelope of the record (interpreted as the instantaneous amplitude of the time history curve) to this quantity. Such relations are based on assumed narrow-band behavior of the energy

spectrum [5], and yield expressions for the mean amplitude of oscillation (half the distance between the trough and crest of an oscillation), the mean of the highest 1/3 of such amplitudes (known as the significant amplitude), and other related statistical parameters of interest for a specified sea condition. In particular the relations for average pitch amplitude and significant pitch amplitude are given by

$$\theta_{av.} = 0.88\sqrt{E_\theta}$$
$$\theta_{sig.} = 1.41\sqrt{E_\theta} \qquad (64)$$

Examples of spectral densities of the heave and pitch motions are given in Figures 19 through 28 , which have been obtained in accordance with the relation of Equation (57). Results were only obtained for Sea States 5 and 6 since very small motions (of no practical consequence) occurred in Sea State 4. Examination of these spectra indicates that the motion characteristics in a given sea state are largest for the lower forward speed and for headings that depart from pure head seas (data only valid up to 45^{o} heading). These conclusions are only valid for unidirectional irregular seas, and the variation with heading is due to the increase of the effective wave spectra (including the Jacobian terms) for the large heading angle β, as can be seen from a comparison of wave spectra in Figures 17 and 18 . Similarly these conclusions are based on the very similar response amplitude characteristics obtained for different heading conditions in this theoretical study. Thus the results for the heave and pitch motion spectra must be checked against experimental data to determine their validity. However, certain conclusions obtained from the theoretical results are still evident, viz. that motions in

unidirectional waves are reduced by heading directly into the waves at the highest possible forward speed. This conclusion is only appropriate for the sea states considered in this study, and it may also be modified by the effects of short-crestedness of the waves, thus limiting its usefulness in determining optimum heading and speed for motion reduction. Since aircraft carriers must operate during the landing phase with a certain required minimum wind-over-deck velocity, the operating conditions of forward speed and local wind (which is also related to sea state) are determined from considerations other than those dictated by ship motion. A sea condition is usually associated with a local wind value, and hence the carrier must experience the particular environment associated with that wind when achieving the required wind-over-deck velocity. Similarly, any local swell conditions in the area of operation will also contribute to the resultant ship motion, and hence the varying complications that relate forward speed, local wind, and local sea conditions preclude any simple means of relating ship motion to a particular set of local environmental conditions (sea and wind).

The results of computations of roll motion, as mentioned previously, indicated extremely small roll amplitudes, and the limited extent of coverage of the frequency domain (for wavelengths up to 2.5 times the ship length) shows that complete response characteristics could not be obtained. However, some attempt was made to extend these curves by analytical techniques in order to allow a determination of roll spectra. The form chosen for representing the roll response operator is given by

$$\frac{\phi}{\eta} = T_{\phi\eta} = 10^{-2} \sin\beta \frac{s}{1 + .202s + 9.951\, s^2} \qquad (65)$$

in transfer function form where $s = i\omega_e$ is substituted in order to obtain the frequency characteristics. Using this information, values of roll spectra were obtained for a number of conditions with larger heading angles, up to beam seas, in order to illustrate the appearance of the resulting spectra. Some of these results are exhibited in Figures 29 through 31, where it can be seen that Sea State 6 results in a much larger spectral response than Sea State 5.

In order to account for the effects of swells, a swell spectrum was arbitrarily developed in a form appropriate to a sharply tuned second order system with small damping, with the spectrum (in terms of the frequency of encounter ω_e) represented by

$$A_s^2(\omega_e) = K_s^2 \frac{\omega_e^2}{\left(1 - \frac{\omega_e^2}{\omega_s^2}\right)^2 + 4\zeta_s^2 \frac{\omega_e^2}{\omega_s^2}} \qquad (66)$$

The swell spectral area is given by

$$E_s = \int_0^\infty A_s^2(\omega_e)d\omega_e = K_s^2 \frac{\pi\omega_s^3}{4\zeta_s} \quad , \qquad (67)$$

and since the significant wave height is given by $\eta_{1/3} = 2.83\sqrt{E_s}$, this determines the value of the gain parameter K_s for a given value of ω_s (center frequency) and ζ_s (the damping factor which determines the sharpness of the swell spectrum). In order to represent the effects of heave motion and pitch motion in swells, it was assumed that the heave and pitch response characteristics were relatively broad in the region of the swell frequency. Thus only a constant multiple (chosen from the response amplitudes at the particular swell center frequency) was selected to multiply the swell transfer function

to represent the basic transfer function for heave, which is given by

$$T_z = \bar{K}_z(\omega_s)\, T_s = \bar{K}_z(\omega_s)\, K_s \frac{s}{1 + 2\zeta_s \frac{s}{\omega_s} + \frac{s^2}{\omega_s^2}} \tag{68}$$

where $\bar{K}_z(\omega_s)$ is the average heave response amplitude in the region near ω_s. The pitch transfer function for swell was constructed in such a way that there would be approximately a 90° phase difference between heave and pitch, and the expression for the pitch transfer function is given by

$$T_\theta = \frac{\bar{K}_\theta(\omega_s)}{\omega_s}\, s\, T_s = \frac{\bar{K}_\theta(\omega_s) K_s}{\omega_s} \frac{s^2}{\left(1 + 2\zeta_s \frac{s}{\omega_s} + \frac{s^2}{\omega_s^2}\right)(1 + s)^2} \tag{69}$$

where $K_\theta(\omega_s)$ is the average pitch response amplitude in the region about ω_s obtained from the amplitude response diagrams. An additional attenuating term was placed in the transfer function denominator to insure attenuation at the larger frequencies. On the basis of the expression for the roll response operator given by Equation (65), the roll transfer function for response to swell is given by

$$T_\phi = T_{\phi\eta}\, T_s = 10^{-2} K_s \sin\beta \frac{s^2}{(1 + .202s + 9.951s^2)\left(1 + 2\zeta_s \frac{s}{\omega_s} + \frac{s^2}{\omega_s^2}\right)} \tag{70}$$

These forms of transfer functions in the standard transfer function variable s are formulated in this manner for aid in the computer simulation and analysis that was carried out by Systems Technology, Inc. [18]. In their case, using an adjoint technique for system analysis, they required the spectra of the ship motions to be represented in the form of an effective shaping filter that operates

on a white noise input of unit amplitude, and the equations for representing the swell effect, as shown above, are appropriate for this purpose.

APPLICATION TO ANALYSIS OF AIRCRAFT CARRIER OPERATIONS

Since the intent of this study was to develop proper representations of aircraft carrier motions at sea, in order to aid in a system analysis of the aircraft carrier landing operation, plans were made to implement an actual representation that would be useful in the computer simulation. A set of representative severe ship motion conditions was established by selecting certain wave systems for analysis by the methods described in the previous sections of this report. The sea conditions were considered to be made up of a storm sea appropriate to Sea State 6, together with a swell corresponding to a center frequency given by $\omega_s = 0.4$, with a 15 ft. significant height. The Sea State 6 storm wave system was assumed to have a 17 ft. significant height, and it was assumed that the heading of the waves was 30° off the bow. Assuming independence of the sea and the swell, the total sea spectra is equal to the sum of the separate spectra of Sea State 6 and the swell, which results in the response spectra being the sum of the spectral responses to each of these separate systems. The resulting rms value of a particular motion, or average value, etc., are determined from the square root of the sum of the squares of the separate response characteristics due to sea and swell taken alone. Since the swell center frequency usually is lower than the band of maximum energy in a sea state, it can be expected that heave motions will be larger in the swell than in a sea, since the response amplitudes indicated in Figures 6, 8 and 10 show a larger heave response at the lower frequency. No definite statement can be made with regard to pitch in this case, but it can be expected that results from both inputs will be commensurate if there is sufficient overlap

of the spectral bands of sea and swell with significant energy through the region of pitch response. With regard to roll, it is expected that the spectral response will be larger for swell, since roll is a sharply tuned motion with a low natural frequency. These combined motions, which are more realistic for operation at sea, were evaluated for a Forrestal class carrier at a forward speed of 10 knots, and the results compared favorably with those obtained from full scale data of the USS Essex [19]. This allowed the use of representative fits of appropriate filter forms to be carried out by Systems Technology, Inc. in order to carry out their system analysis of the aircraft carrier landing operation (see [18] for details of the simulation and their results on landing operations).

The evaluation of any spectral response for a particular desired operational condition, either sea or swell or their combination, can be carried out in the manner outlined above using all of the basic data developed in this study. The major use of these results in the landing analysis has been restricted to the heave and pitch data, since the roll effect does not appreciably affect terminal landing dispersions [18]. As discussed earlier, the basic conditions established at sea for a landing operation require a specific wind-over-deck velocity, and the ship must necessarily adapt to the environment that is present during the particular time of the aircraft operations. The limits of ship motion that will interfere with the aircraft carrier landing operation are a pitch motion of the order of $\pm 1.5^{o} - 2^{o}$, which is not a large motion per se. However, for a ship of the Forrestal class a $\pm 2^{o}$ pitch angle results in the stern ramp varying its up and down motion through a height range of 35 ft., and it can be seen that such a motion will certainly limit the effectiveness of aircraft

landing operations. Thus the ship motion limits in various sea states should be established in order to determine the influence of these motions on the landing operation, which is the intent of [18] and subsequent analyses.

Another application of the ship motion data which is essential for proper analysis of motion influence in the landing operation is for determining the effective kinematics of the FLOLS beam due to the influence of the various ship motions, and also the required stabilization technique for the lens unit itself. A detailed analysis of the kinematics is presented in [18], where the distances to the lens location are referred to the effective "center" of pitch and the effective "center" of roll. These locations are not fixed points on the ship, but vary over a range of positions during a motion time history. Actually the pitching axis is supposedly located at a point which has "zero" acceleration, or at the point of minimum vertical motion [20]. Since these locations are not precise, it appears to be more useful to refer to a better reference point, and if the ship motions determined from the present analysis are used, then the appropriate reference point for the resultant ship motions should be the center of gravity of the ship. While that location may be difficult to select also because of different loadings on a ship at different times, it is certainly more realistic and there is a greater reliability since the CG location can be related to the location of the center of buoyancy (CB), which determines the ship trim conditions.

The information obtained herein is only appropriate to aircraft carriers of the Forrestal class, but it is possible to obtain some information on other carriers from this data, within certain limits. The technique for extending

these results to a smaller carrier class (such as that of the Midway class) is to assume that the responses of the ships will be the same for the same ratios of wavelength to ship length, i.e. $\frac{\lambda}{L}$. This is then converted to the appropriate frequencies of encounter for the other class, taking account of forward speed and direction, etc., and a response amplitude and phase can be obtained in this manner. However, this equivalence of similar response for the same values of $\frac{\lambda}{L}$ will not necessarily carry over to other ships because the natural periods of the motions of heave, pitch, and roll are important in determining particular ship responses. Since these periods do not necessarily scale by simple linear relationships in terms of length ratios, there may be some differences in the results. However, this approach may still be useful as a first approximation.

In addition to the use of the results obtained in this study for simulation purposes in a system analysis, there are a number of other possible applications. The data obtained herein is necessary for determining the stabilization effort required if devices such as anti-pitching fins are considered to be installed on carriers for the purpose of ship motion reduction. The basic environment data is important also for the actual development of automatic landing systems for carriers, since it outlines the environmental characteristics at sea, which must be used to develop specifications for system performance. With the recent installation of inertial guidance and navigation systems on board carrier-based aircraft, it is necessary to carry out proper alignment of the inertial systems while on board the carrier. The information on ship motion contained herein will be useful for providing data appropriate to that particular operation. Another significant application of these results is for determining the required theoretical "building blocks" for development of methods

that would allow prediction of the motion time history. It is intended to proceed with this last approach since it appears to provide a significant pay-off in increased performance during landing operations [18].

CONCLUSIONS AND RECOMMENDATIONS

The main result of this study is a mathematical model which yields a useful representation of aircraft carrier motions at sea for purposes of computer simulation studies, which are necessary for a complete system analysis of aircraft carrier landing operations at sea. While the precise numerical results have not been completely verified by comparison with experiments, a limited comparison with unpublished and preliminary data exhibits good agreement for pitch motion and poorer agreement for the case of heave. Since the pitch motion results in larger vertical deck excursions, which are more significant in the carrier landing problem, the data developed herein provides useful information on the most significant aspect of ship behavior at sea for this particular problem.

With regard to the detailed results of the theoretical computations, the frequency response characteristics (amplitude and phase) using the constant coefficient model are sufficiently close to the responses obtained by use of the standard frequency-dependent coefficient technique. This approach allows computational simplicity and more insight into the basic ship dynamic characteristics (roots of the system characteristic equation which exhibit the natural frequencies and damping ratios for coupled motions). Another feature of the results is limited dependence on heading angle of the frequency response characteristics of a large aircraft carrier, when presented as a function of the frequency of encounter ω_e. This result may have significance with regard to the influence of wave directionality properties on the ship responses. In view of these

various findings, it is recommended that these results be checked with experimental data when such data becomes completely available. It appears plausible that the present theory (if it is fairly representative of actual experimental values) can be used in conjunction with experimental data to provide guidance in determining the response characteristics of an aircraft carrier for a large range of operating conditions. This information should be applied to determine the trends in the significant variables (such as speed, heading angle, etc.) that will yield minimum ship motions for other sea conditions than those considered in the present study. In particular, this information should be applied to real spectra that have been measured at sea (for more severe conditions) in order to determine operational limits.

The information available in the present report on ship response characteristics in waves should be used for developing techniques for motion time history prediction. Since transfer functions, spectral data, etc. are basic elements in prediction theory, this appears to be a natural extension of the results contained in this report. It is recommended that an investigation of the various techniques for time history prediction of ship motion be carried out, with attendant model tests in order to check the effectiveness of the various approaches. The prediction time requirements should certainly be related to the minimum time required for specific aircraft maneuvers during landing. Similarly, it is important to develop some means of implementation of the prediction information into the landing system procedure to obtain the maximum benefits. It is expected that such a program, if successful in attaining accurate prediction for the

proper time interval, will yield significant improvements in the safety and performance of carrier landing operations.

REFERENCES

1. Giordano, M. J., and Linder, P. S.: "Derivation of Roll and Pitch Correction Factors for the Point-in-Space Stabilization Used with Either the Mirror or Fresnel Lens Optical Landing System", Naval Air Material Center Rept.NAEL-ENG-6865, 12 April 1962.

2. "Fresnel Lens Optical Landing System Mk 6 Mod 0, Technical Manual, Installation, Service, Operation and Maintenance Instructions", NavWeps 51-40ABA-1, 15 July 1962.

3. Korvin-Kroukovsky, B. V. and Jacobs, W. R.: "Pitching and Heaving Motions of a Ship in Regular Waves", Transactions, SNAME, 1957.

4. Kaplan, Paul: "Application of Slender Body Theory to the Forces Acting on Submerged Bodies and Surface Ships in Regular Waves", Journal of Ship Research, November 1957.

5. St. Denis, M. and Pierson, W. J.: "On the Motions of Ships in Confused Seas", Transactions, SNAME, 1953.

6. Pierson, W. J., Neumann, G. and James, R. W.: "Practical Methods for Observing and Forecasting Ocean Waves by Means of Wave Spectra and Statistics", U. S. Navy Hydrographic Office Pub. No. 603, 1954.

7. Letter from Dept. of Navy, Bureau of Ships, concerning hull lines for aircraft carriers, 19 July 1963, CVA/9010 Ser 420-273.

8. Faired Lines and Mold Loft Offsets, Bureau of Ships Drawing No. CVA59, SO500, 1465602, Rev. A, 1955.

9. Letter from David Taylor Model Basin with data for aircraft carrier parameters, (585:RW:sb), 25 July 1963.

10. Grim, O.: "Die Schwingungen von schwimmenden, zweidimensionalen Korpern", Hamburgische Schiffbau-Versuchsanstalt Gesellschaft Rpt. 1172, September 1959.

11. Kaplan, Paul and Hu, Pung Nien: "Virtual Mass and Slender Body Theory for Bodies in Waves", Proc. of the Sixth Midwest Conference on Fluid and Solid Mechanics, Univ. of Texas, September 1959.

12. Hu, Pung Nien: "Lateral Force and Moment on Ships in Oblique Waves", Journal of Ship Research, June 1962, Vol. 6, No. 1.

13. Discussion with personnel of Systems Technology, Inc. concerning aircraft carrier motion simulation, Los Angeles, Calif. Feb. 3, 1964.

14. Etkin, Bernard, Dynamics of Flight, Stability and Control, New York, John Wiley and Sons, Inc., 1959.

15. Aircraft carrier model tests in waves at M.I.T., August 1964.

16. Vassilopoulos, Lyssimachos: "The Analytical Prediction of Ship Performance in Random Seas, Including a New Correlation of Theoretical and Experimental Model Motions in Regular Waves", M.I.T. Dept. of Naval Architecture & Marine Eng., Feb. 1964.

17. Vassilopoulos, Lyssimachos and Mandel, Philip: "A New Appraisal of Strip Theory", paper to be presented at 5th Naval Hydrodynamics Symposium, Bergen, Norway, Sept. 1964.

18. Durand, Tulvio S. and Teper, Gary L.: "An Analysis of Terminal Flight Path Control in Carrier Landing", Systems Technology, Inc. Tech. Rept. No. 137-1, August 1964.

19. Jasper, N. H.: "Statistical Distribution Pattern of Ocean Waves and of Wave-Induced Ship Stresses and Motions, with Engineering Applications", DTMB Rept. 921, October 1957.

20. Szebehely, V. G.: "Apparent Pitching Axis", Forschungsheft für Schiffstechnik, Vol. 3, No. 16(1956).

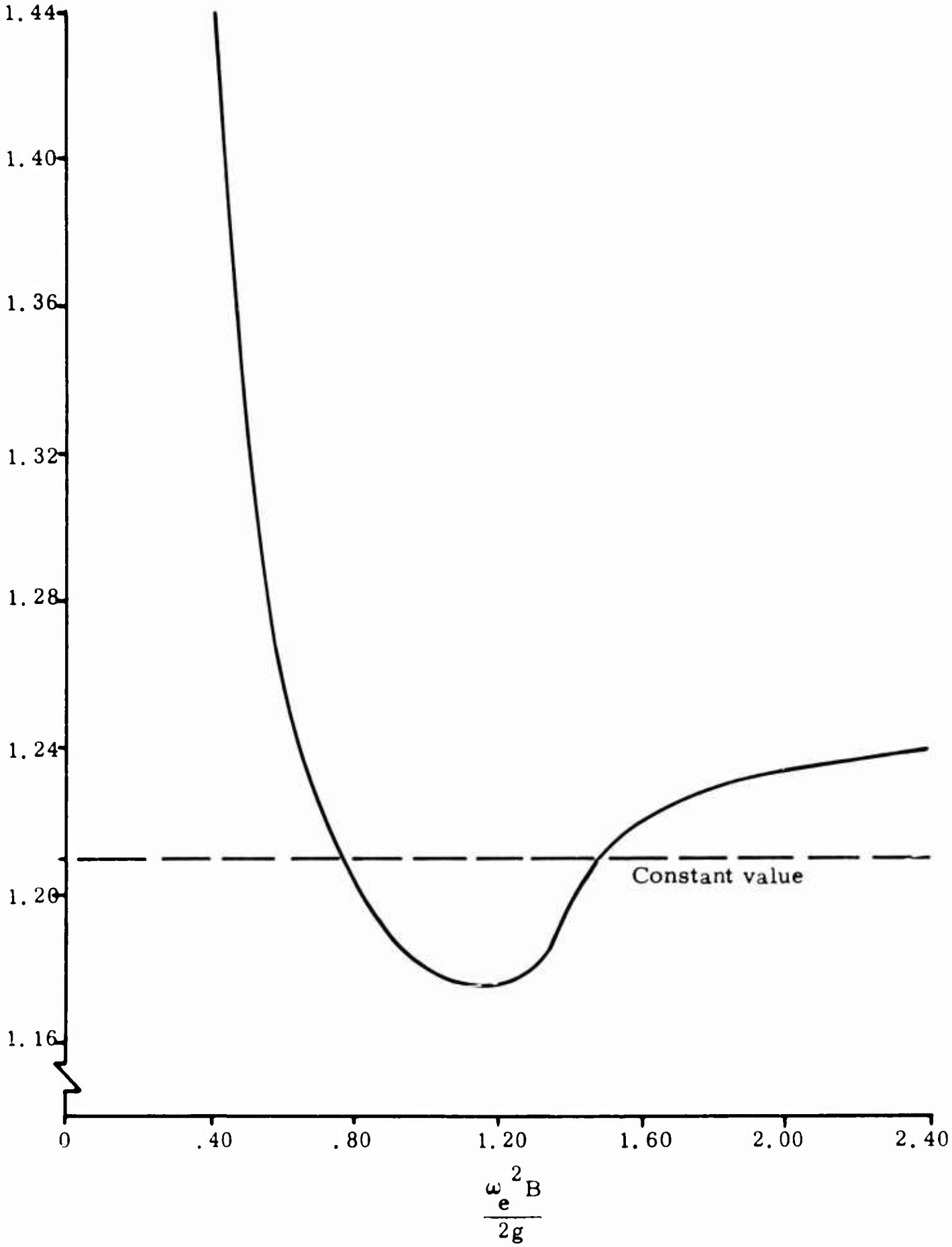

Fig. 1 Added mass as a function of frequency

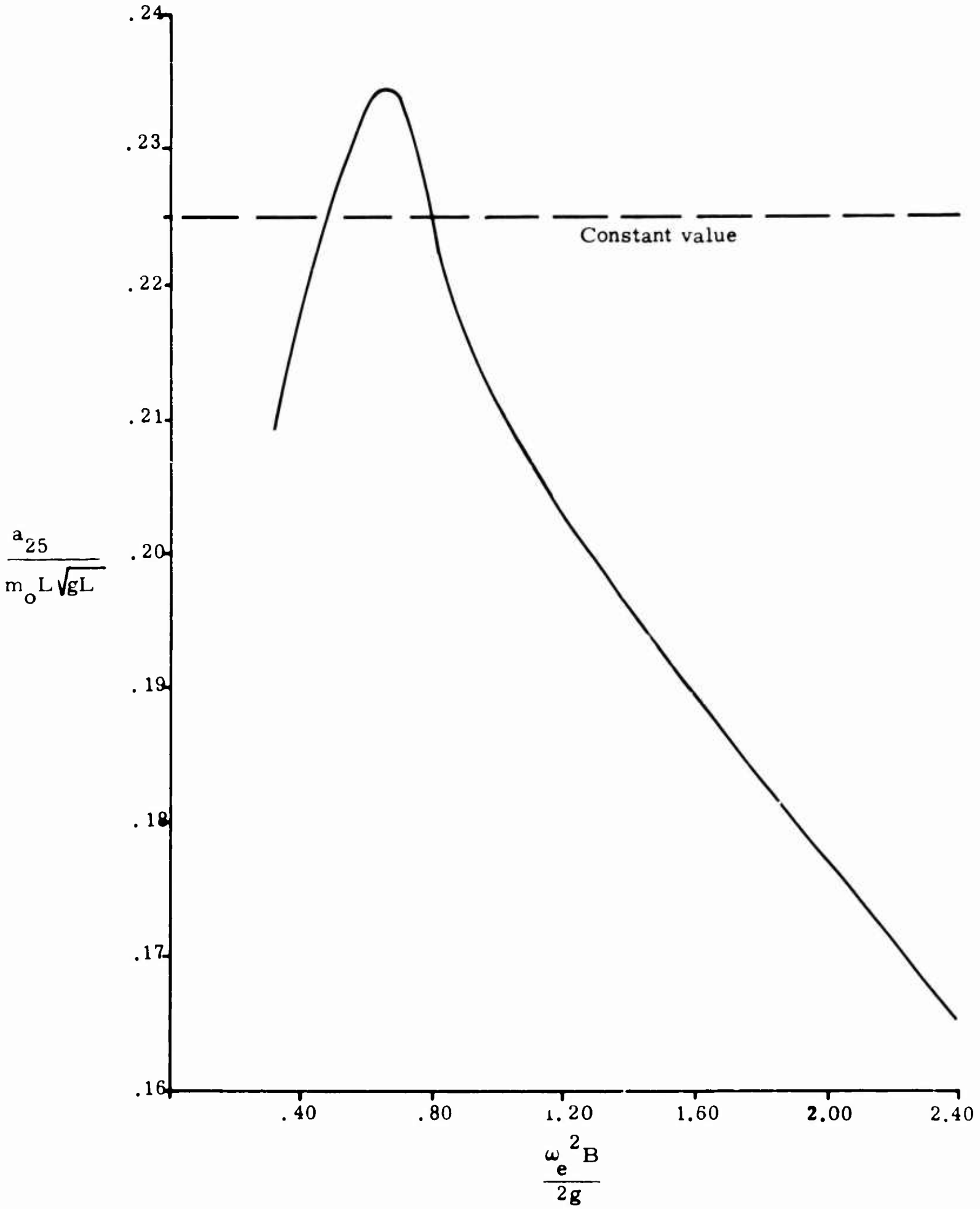

Fig. 2 Pitch damping as a function of frequency

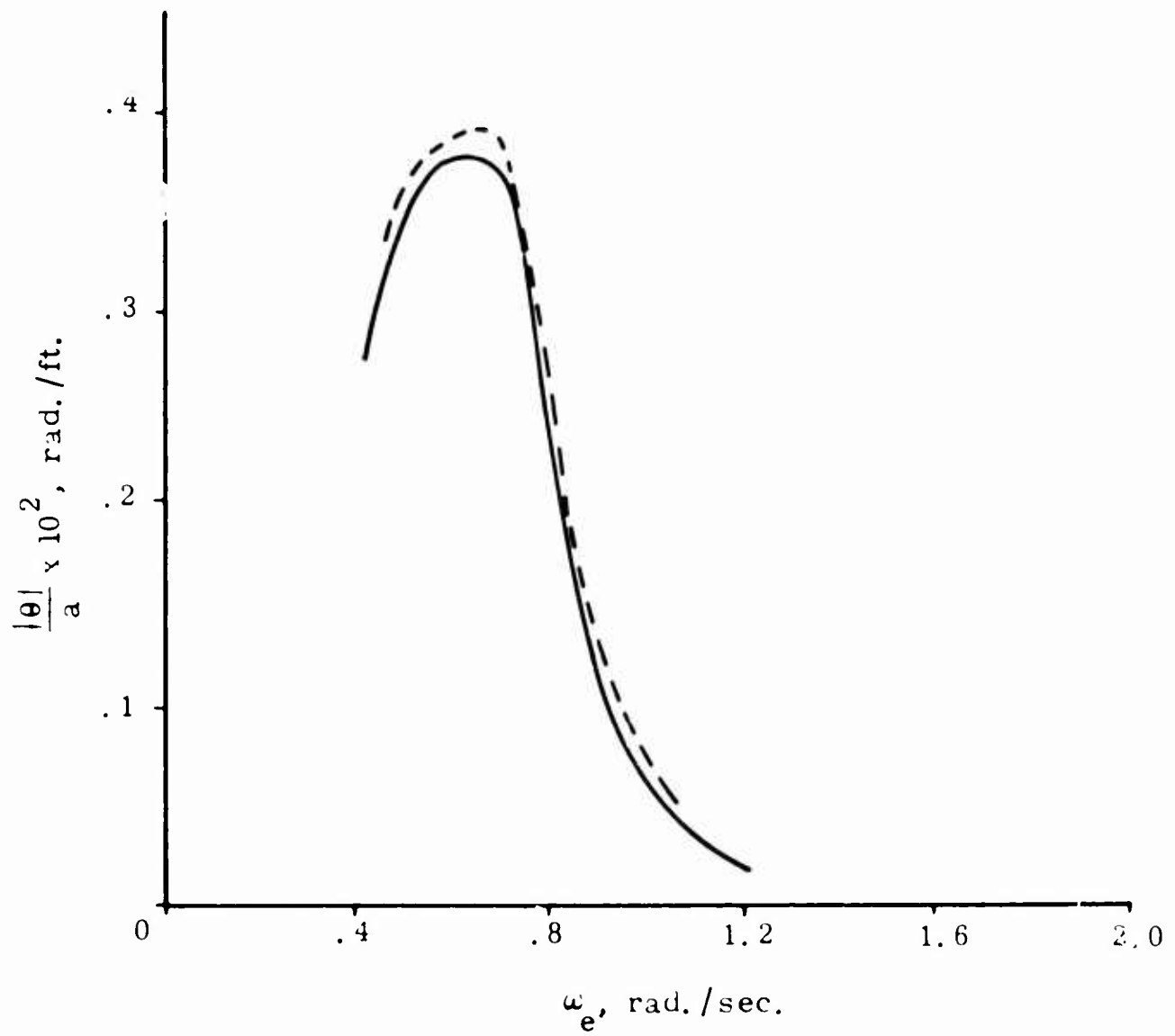

Fig. 3 Comparison of pitch amplitudes using frequency dependent coefficients and constant coefficients

V = 20 knots, $\beta = 0^{\circ}$

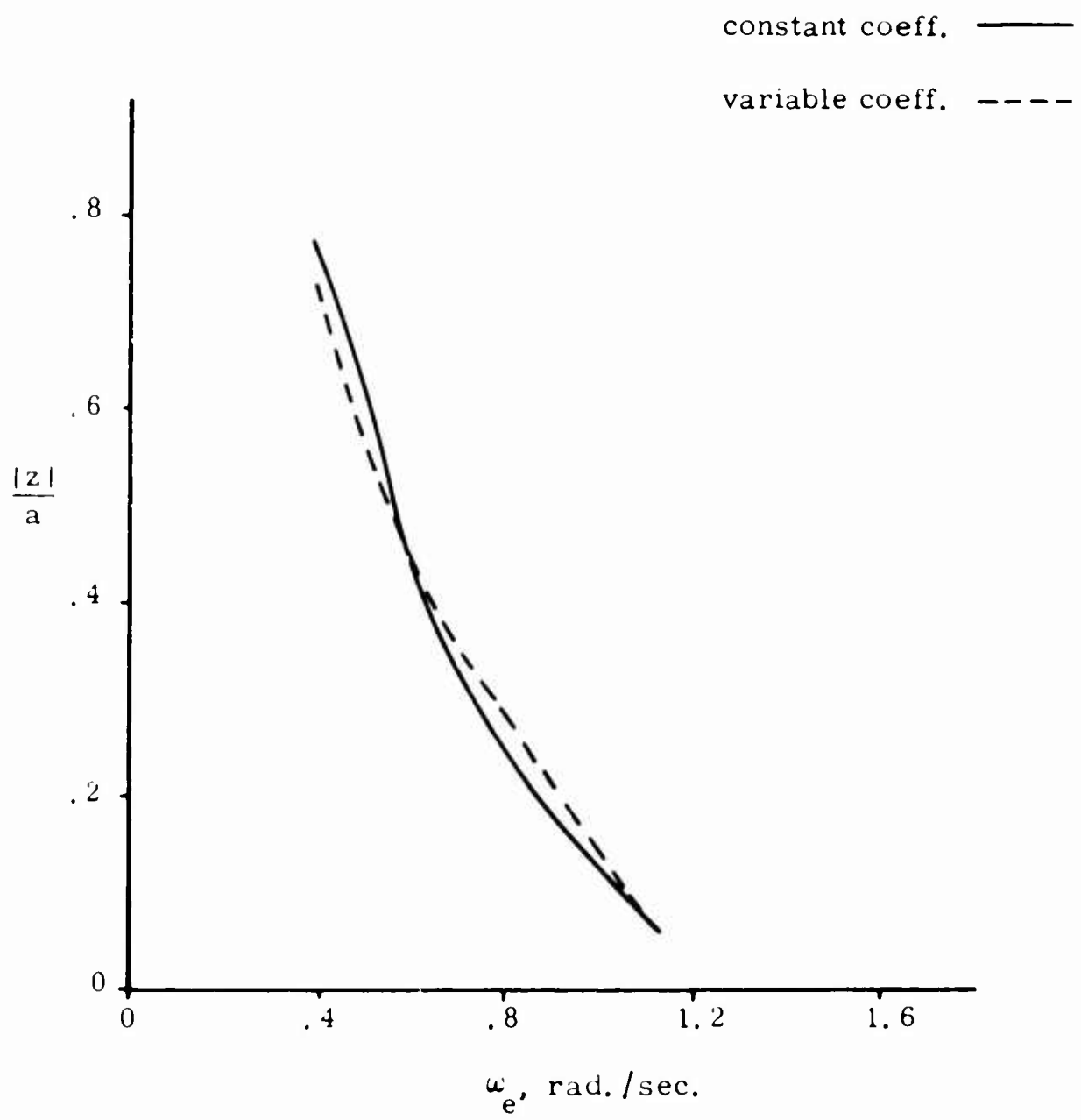

Fig. 4 Comparison of heave amplitudes using frequency dependent coefficients and constant coefficients

V = 10 knots

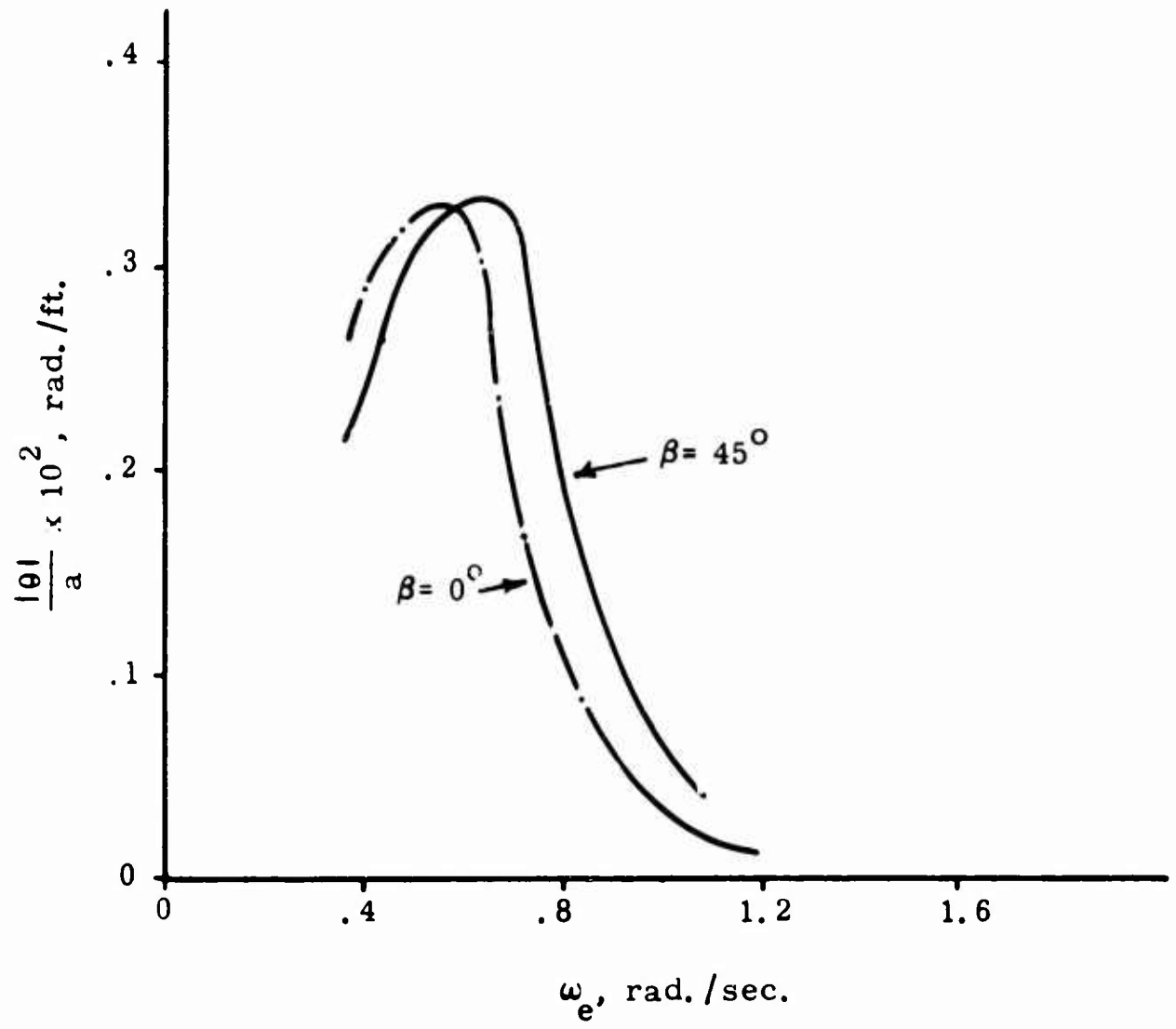

Fig. 5 Pitch amplitude variation with encounter frequency and heading, V = 10 knots

V = 10 knots

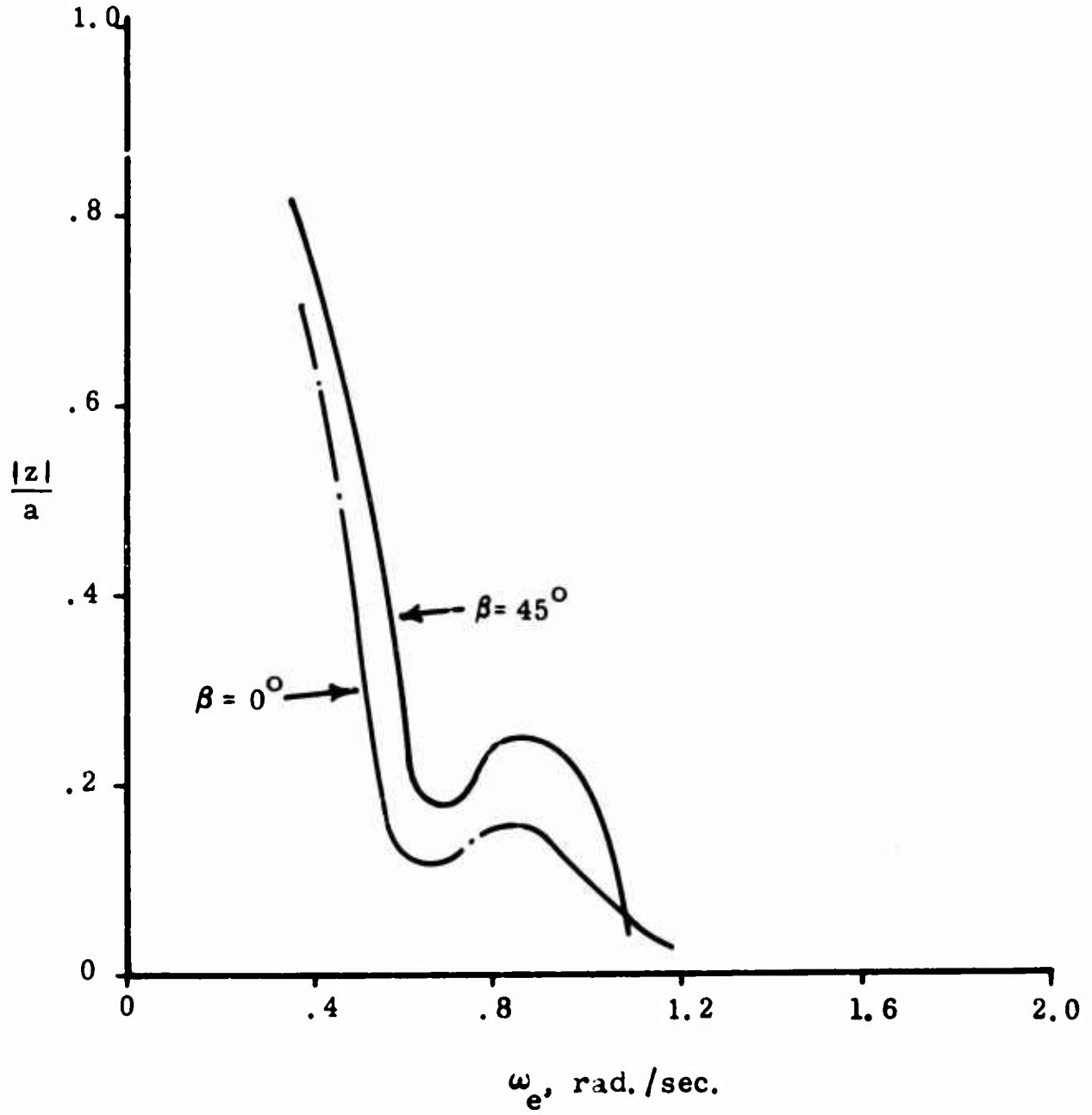

Fig. 6 Heave amplitude variation with encounter frequency and heading, V = 10 knots

V = 20 knots

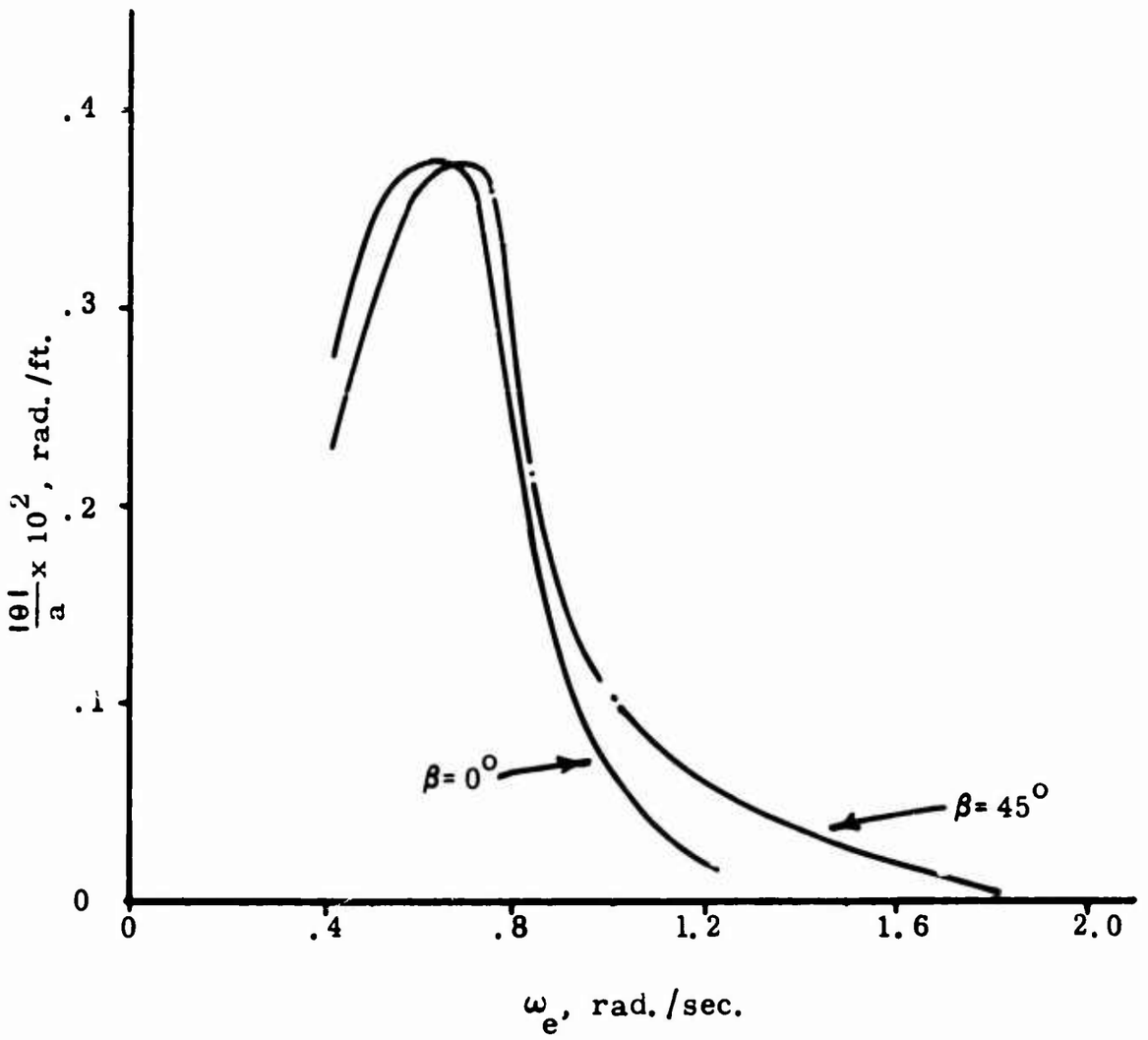

Fig. 7 Pitch amplitude variation with encounter frequency and heading, V = 20 knots

V = 20 knots

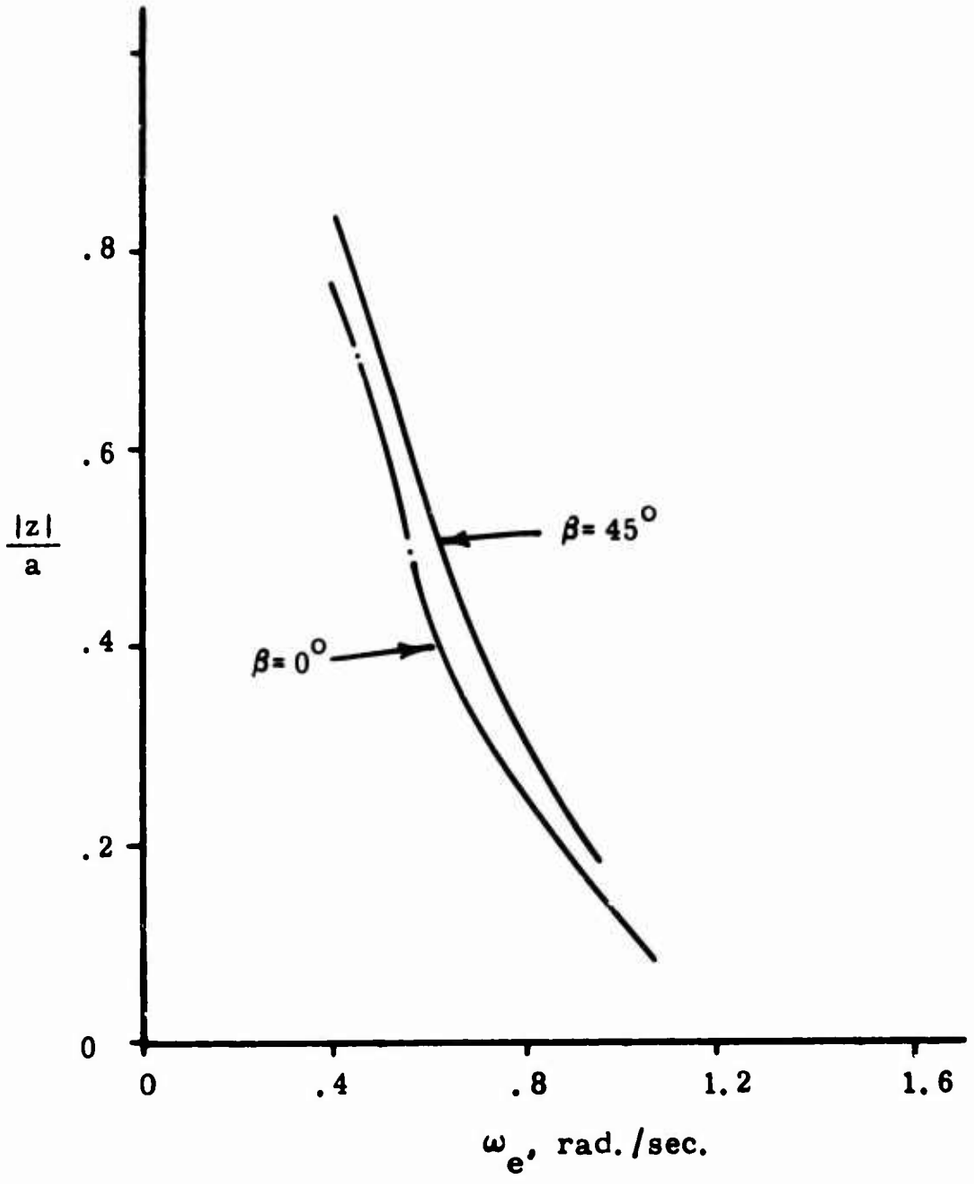

Fig. 8 Heave amplitude variation with encounter frequency and heading, V = 20 knots

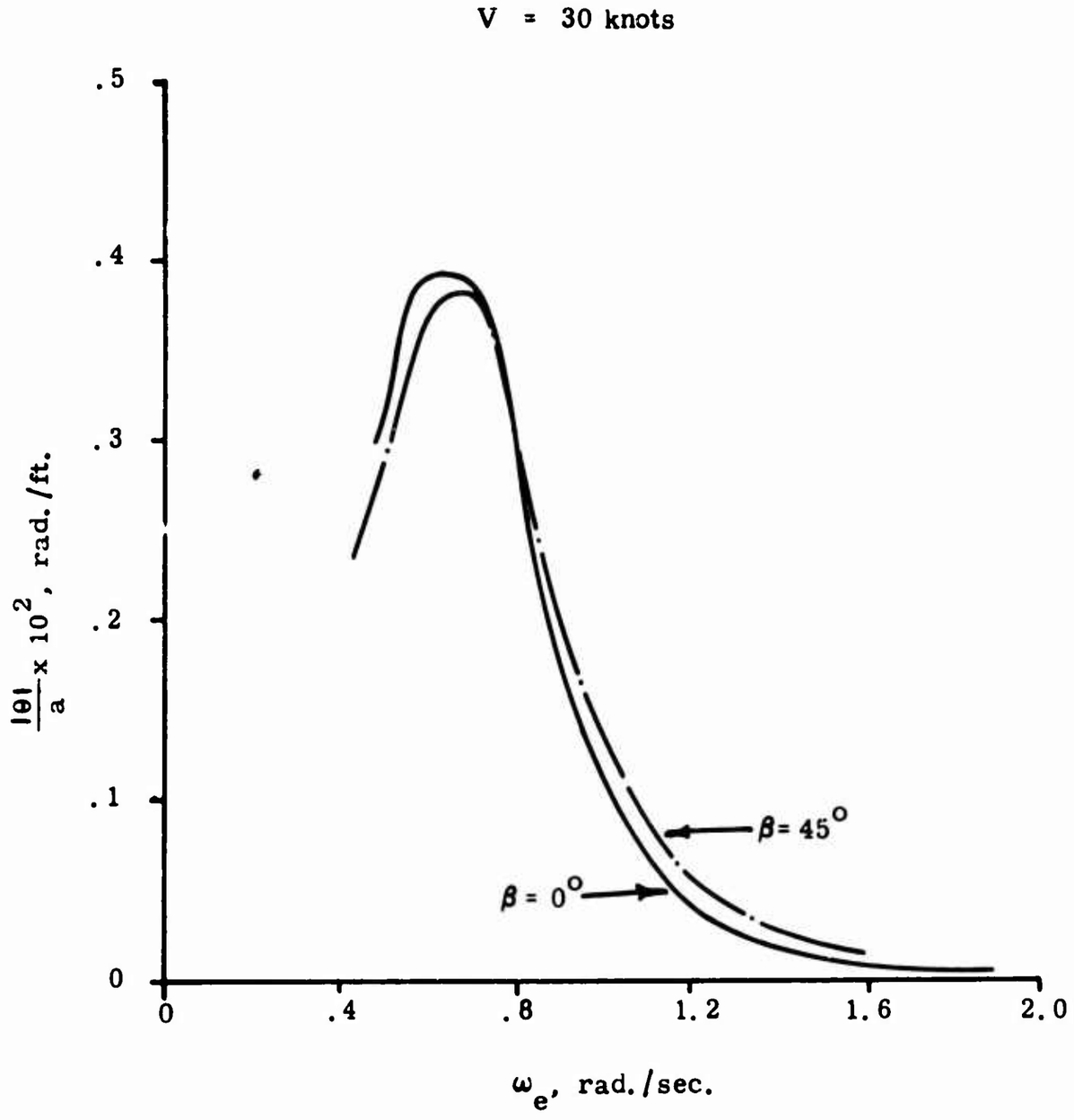

Fig. 9 Pitch amplitude variation with encounter frequency and heading, V = 30 knots

V = 30 knots

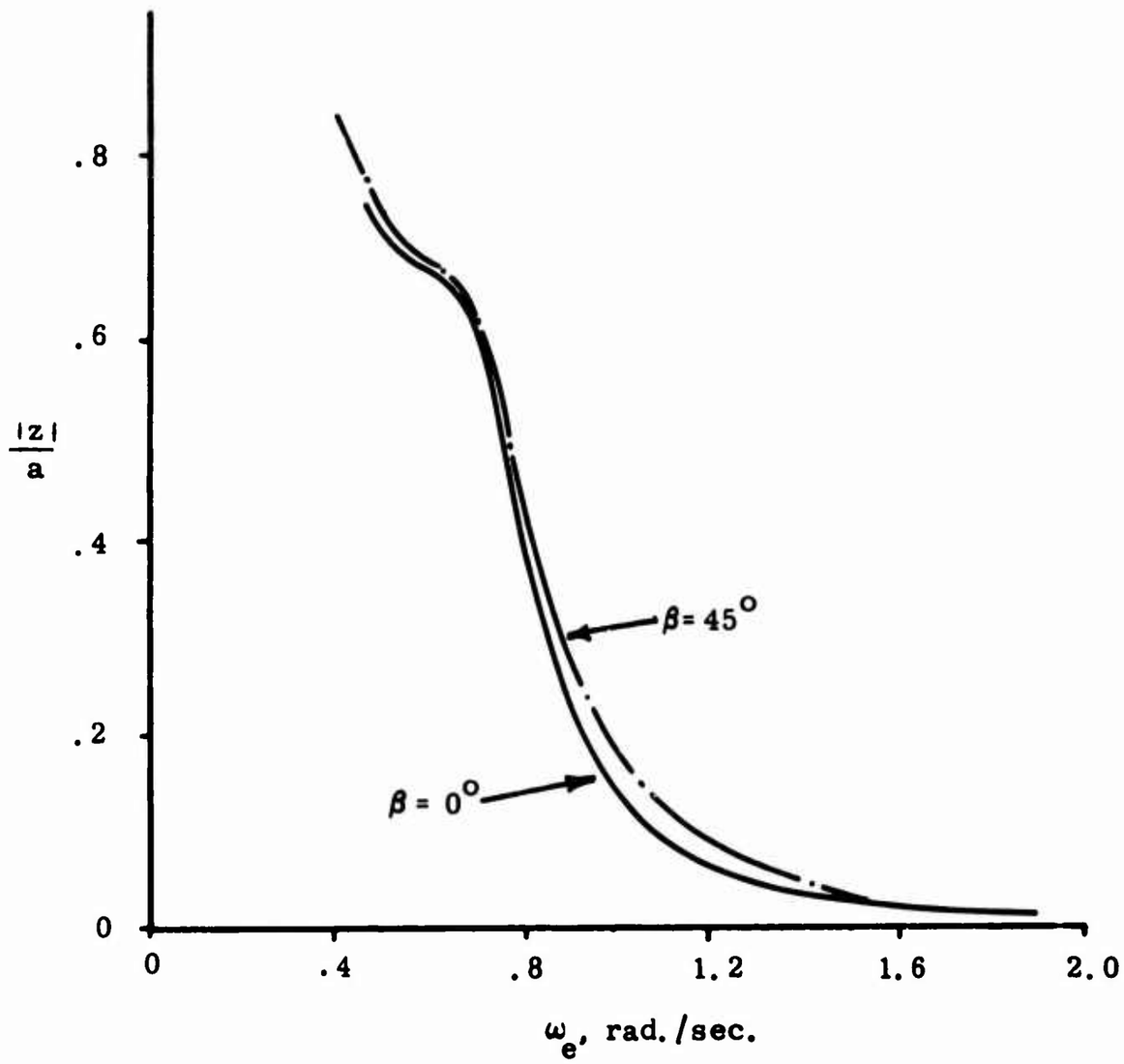

Fig. 10 Heave amplitude variation with encounter frequency and heading, V = 30 knots

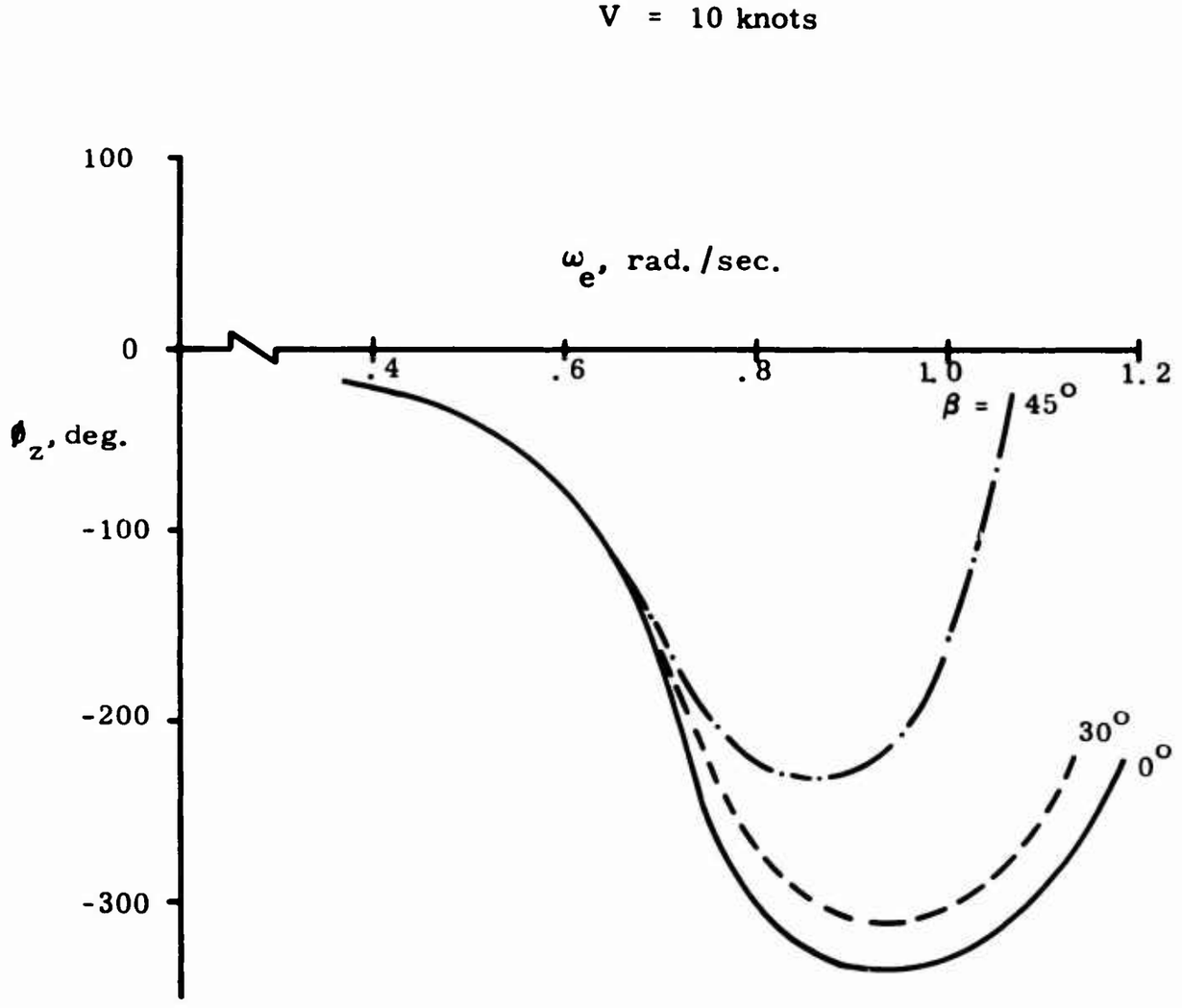

Fig. 12 Variation of heave phase angle with encounter frequency and heading, V = 10 knots

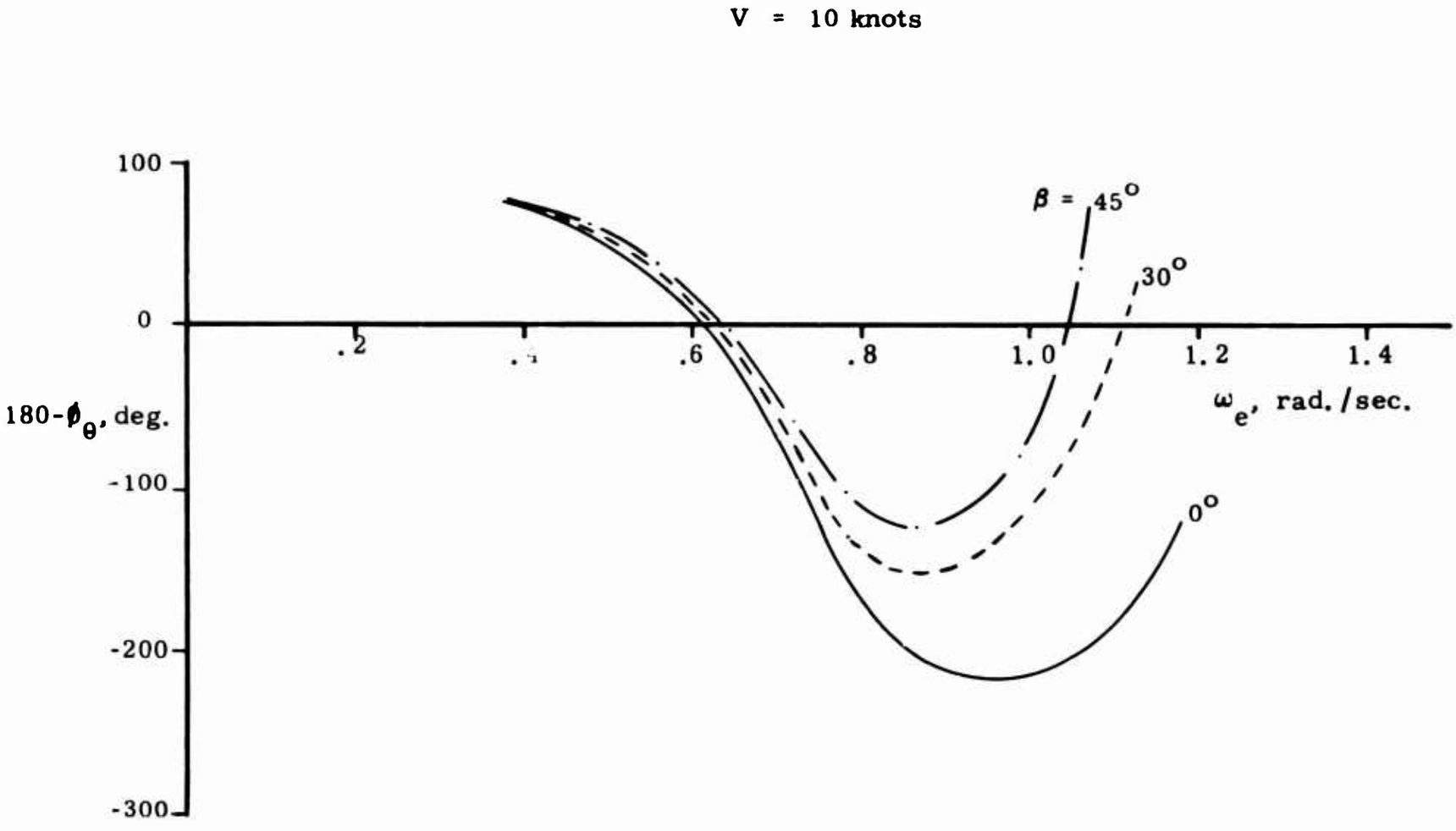

Fig. 11 Variation of negative pitch (- θ) phase angle with encounter frequency and heading, V = 10 knots

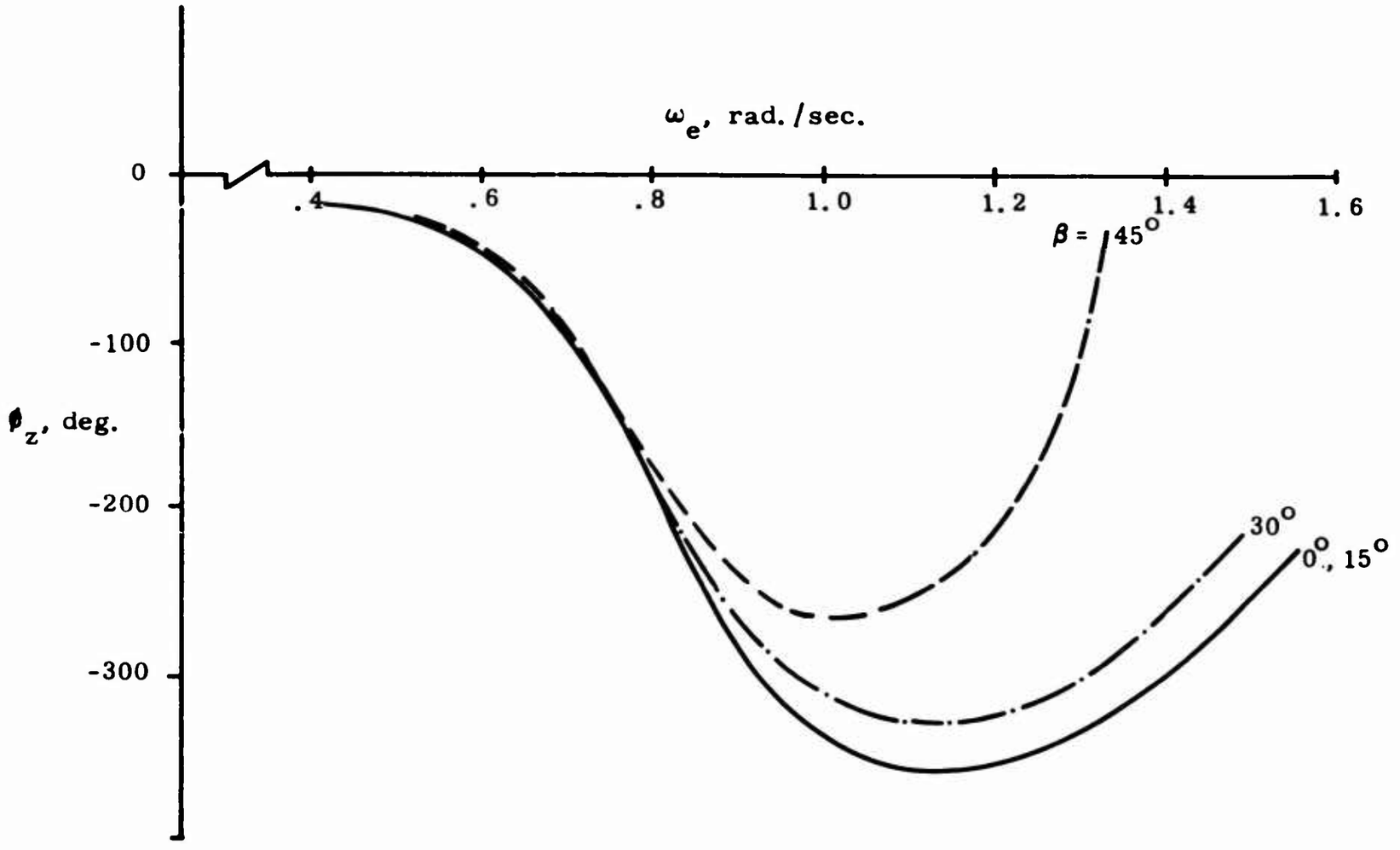

Fig. 14 Variation of heave phase angle with encounter frequency and heading, V = 20 knots

V = 20 knots

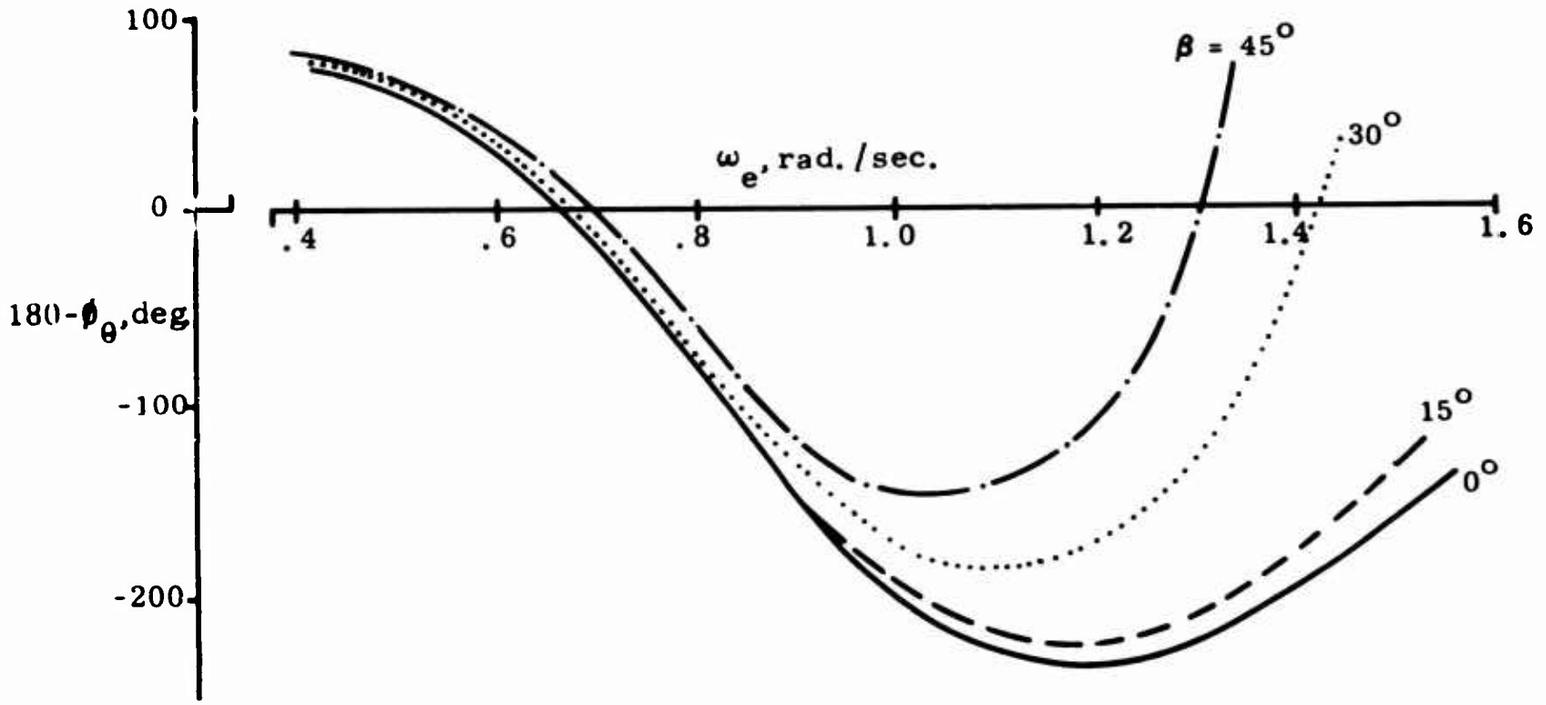

Fig. 13 Variation of negative pitch (- θ) phase angle with encounter frequency and heading, V = 20 knots

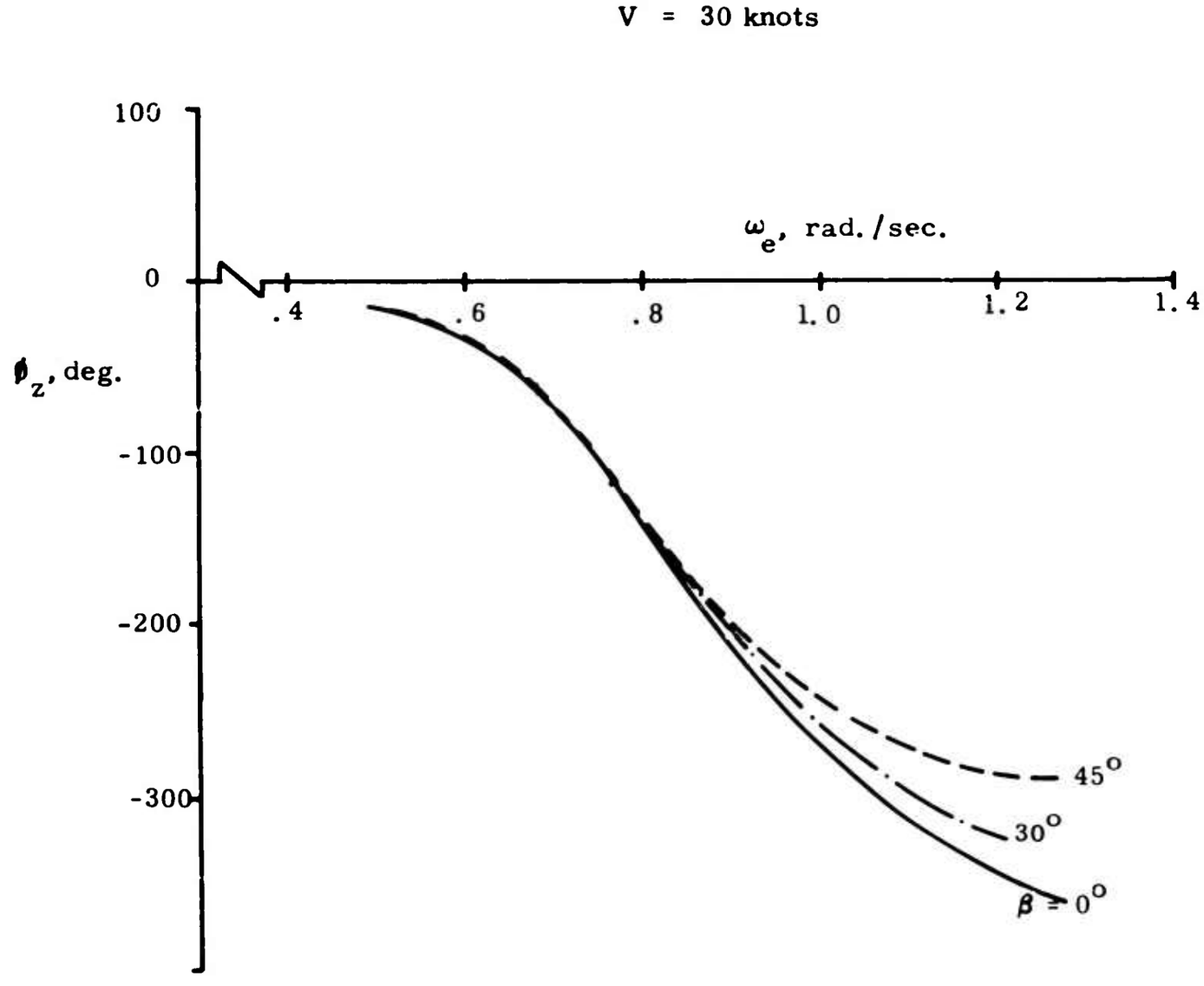

Fig. 16 Variation of heave phase angle with encounter frequency and heading, V = 30 knots

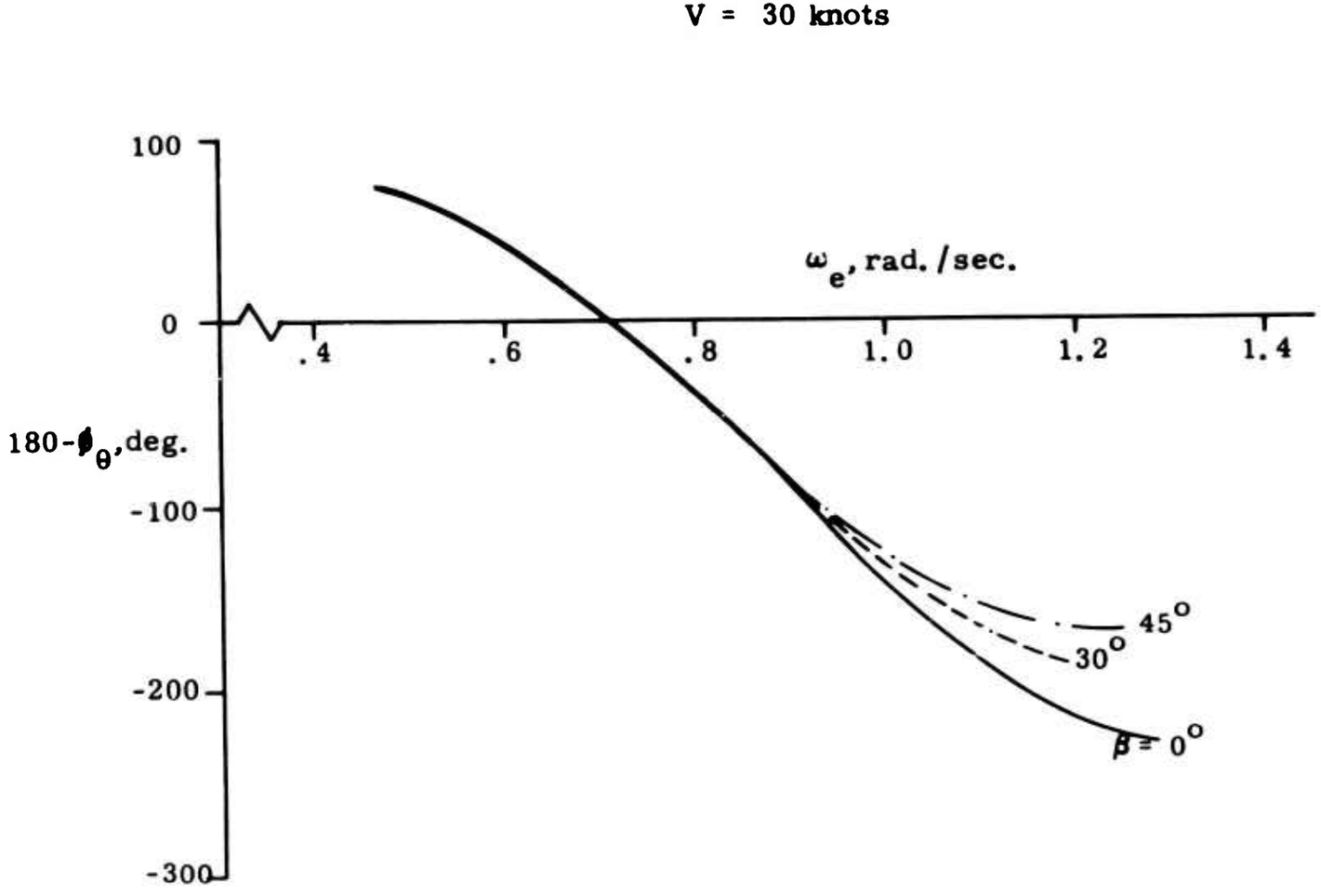

Fig. 15 Variation of negative pitch (- θ) phase angle with encounter frequency and heading, V = 30 knots

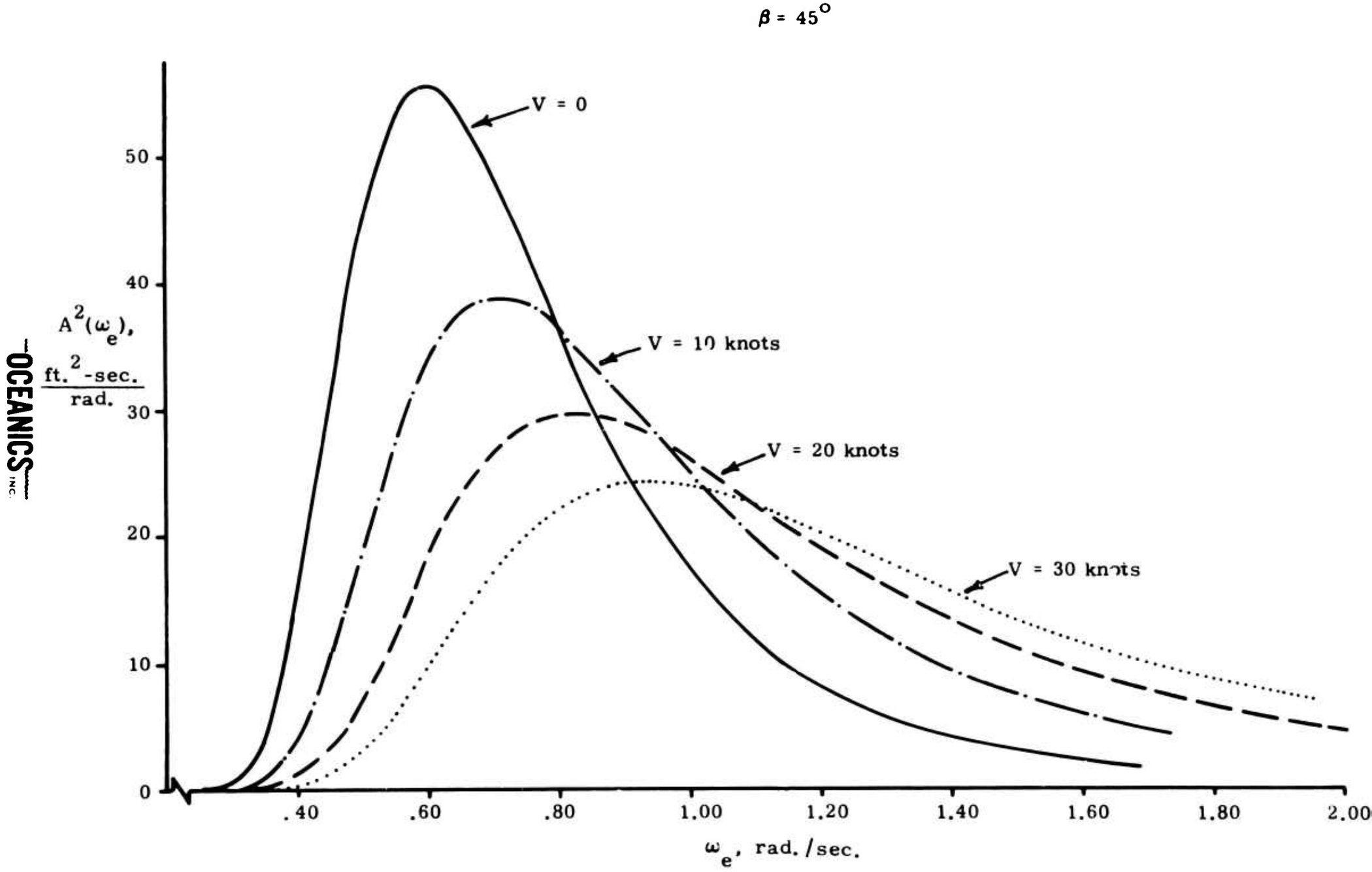

Fig. 18 Effective wave spectrum for unidirectional Sea State 6, $\beta = 45^{\circ}$

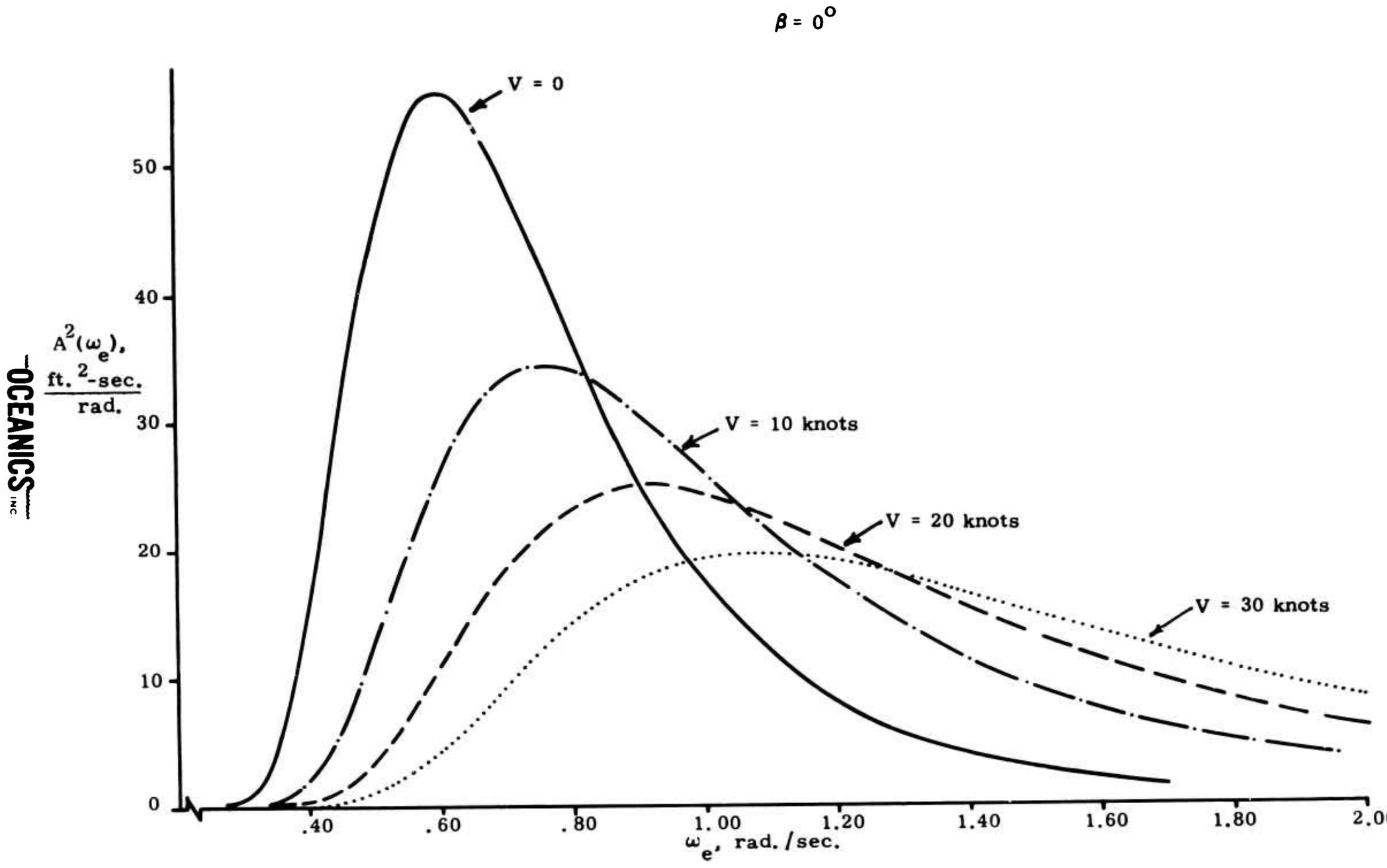

Fig. 17 Effective wave spectrum for unidirectional Sea State 6, $\beta = 0^{o}$

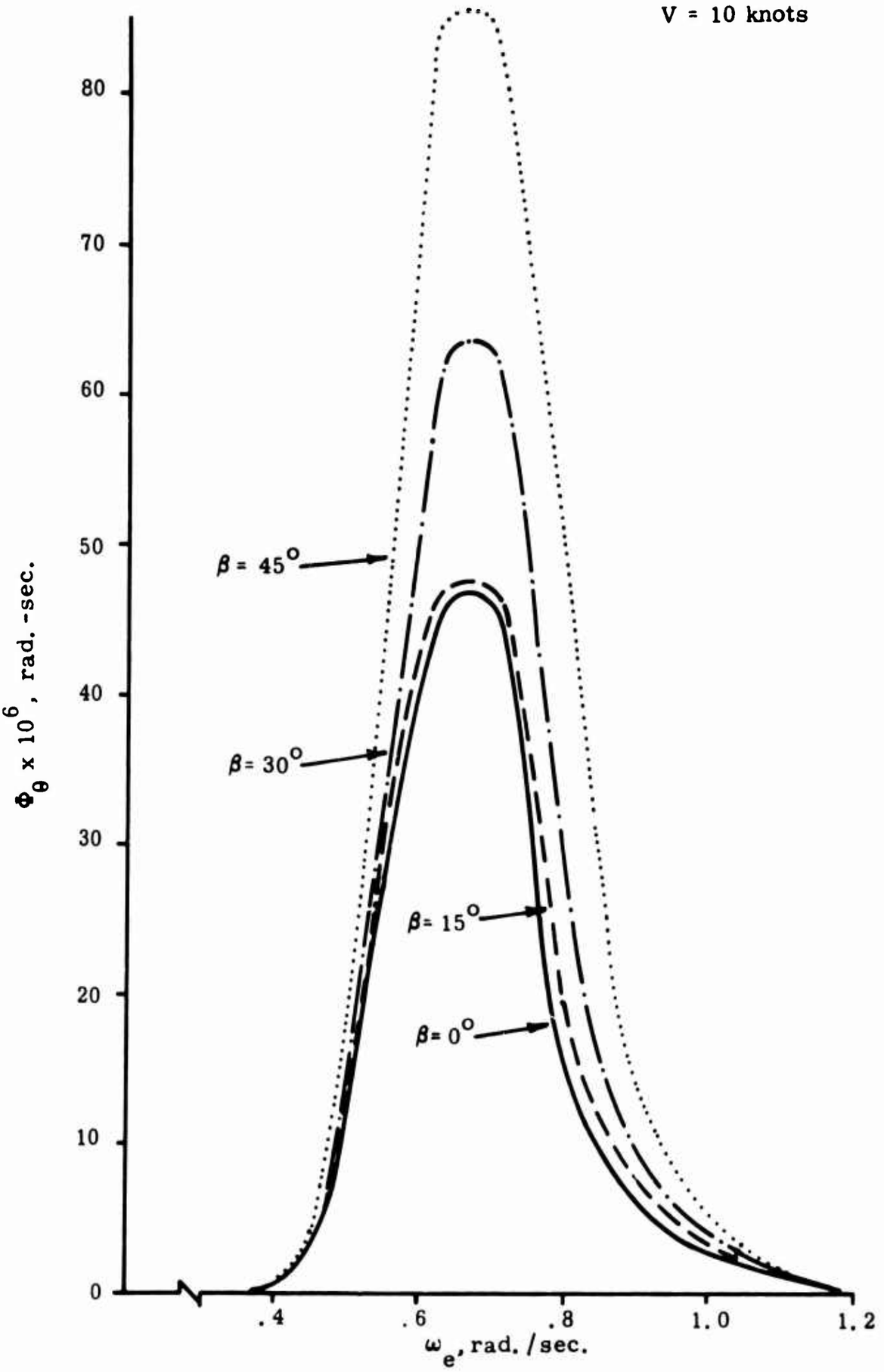

Fig. 19 Pitch spectrum in unidirectional Sea State 5, V = 10 knots

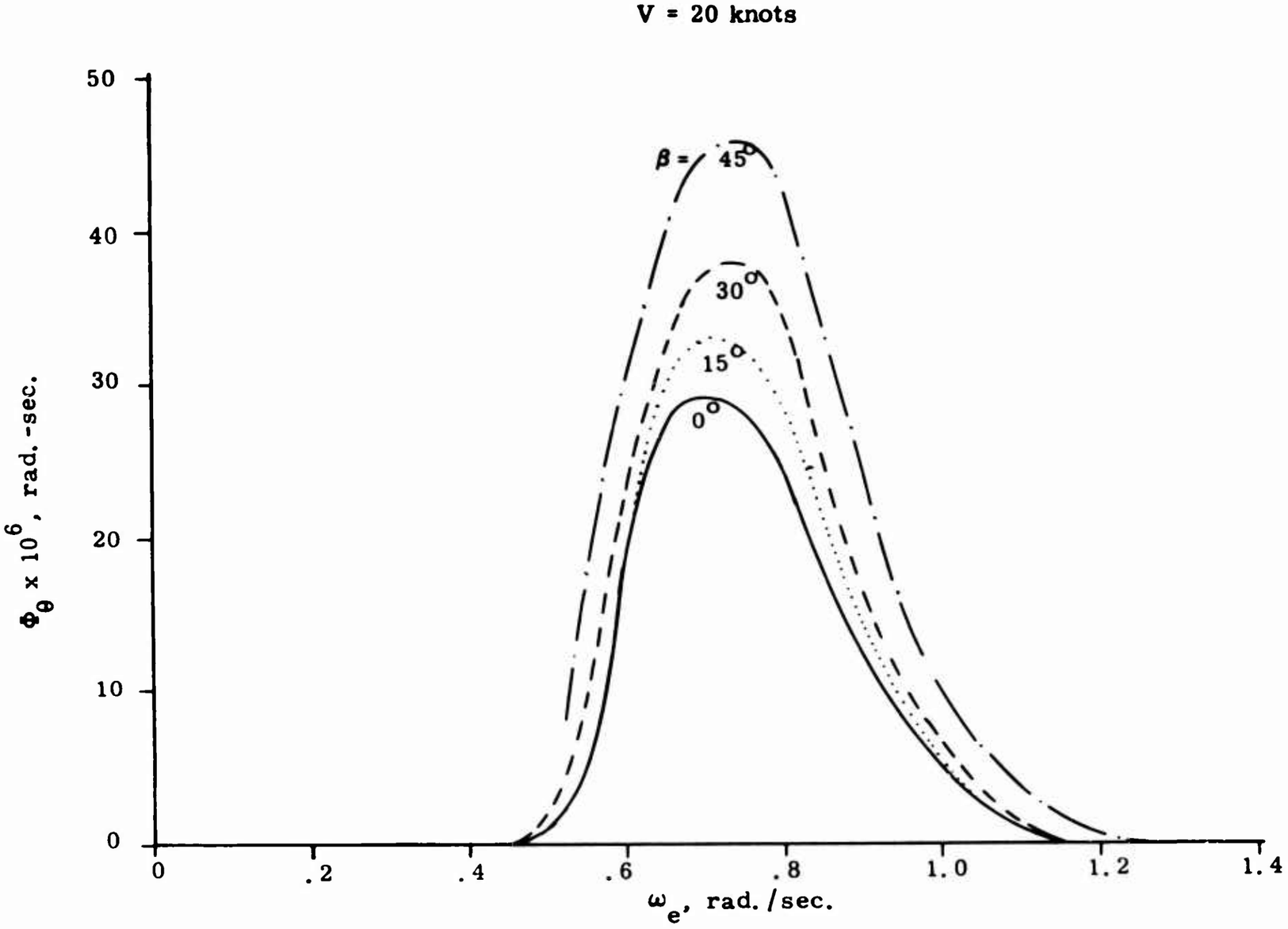

Fig. 20 Pitch spectrum in unidirectional Sea State 5, V = 20 knots

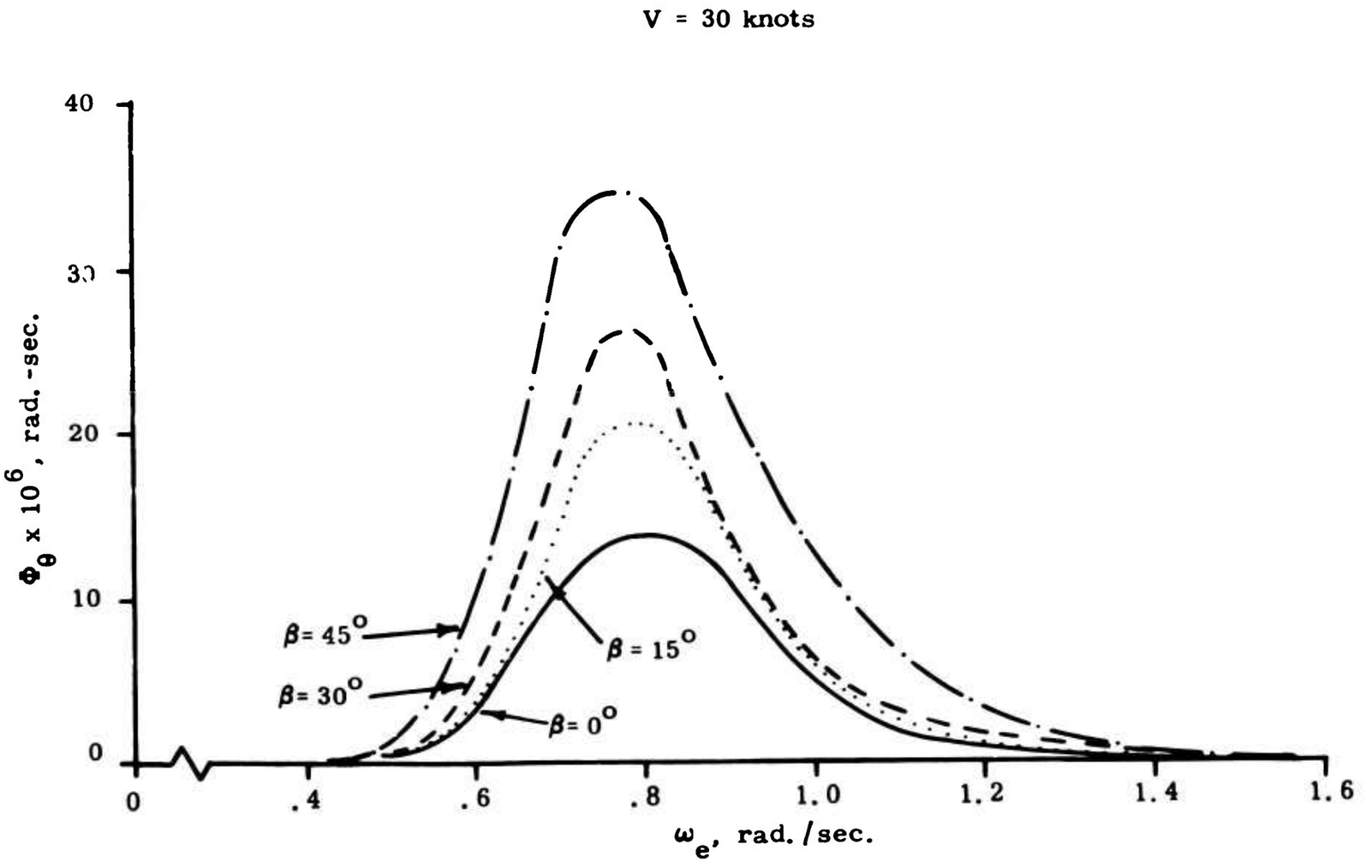

Fig. 21 Pitch spectrum in unidirectional Sea State 5, V = 30 knots

V = 10 knots

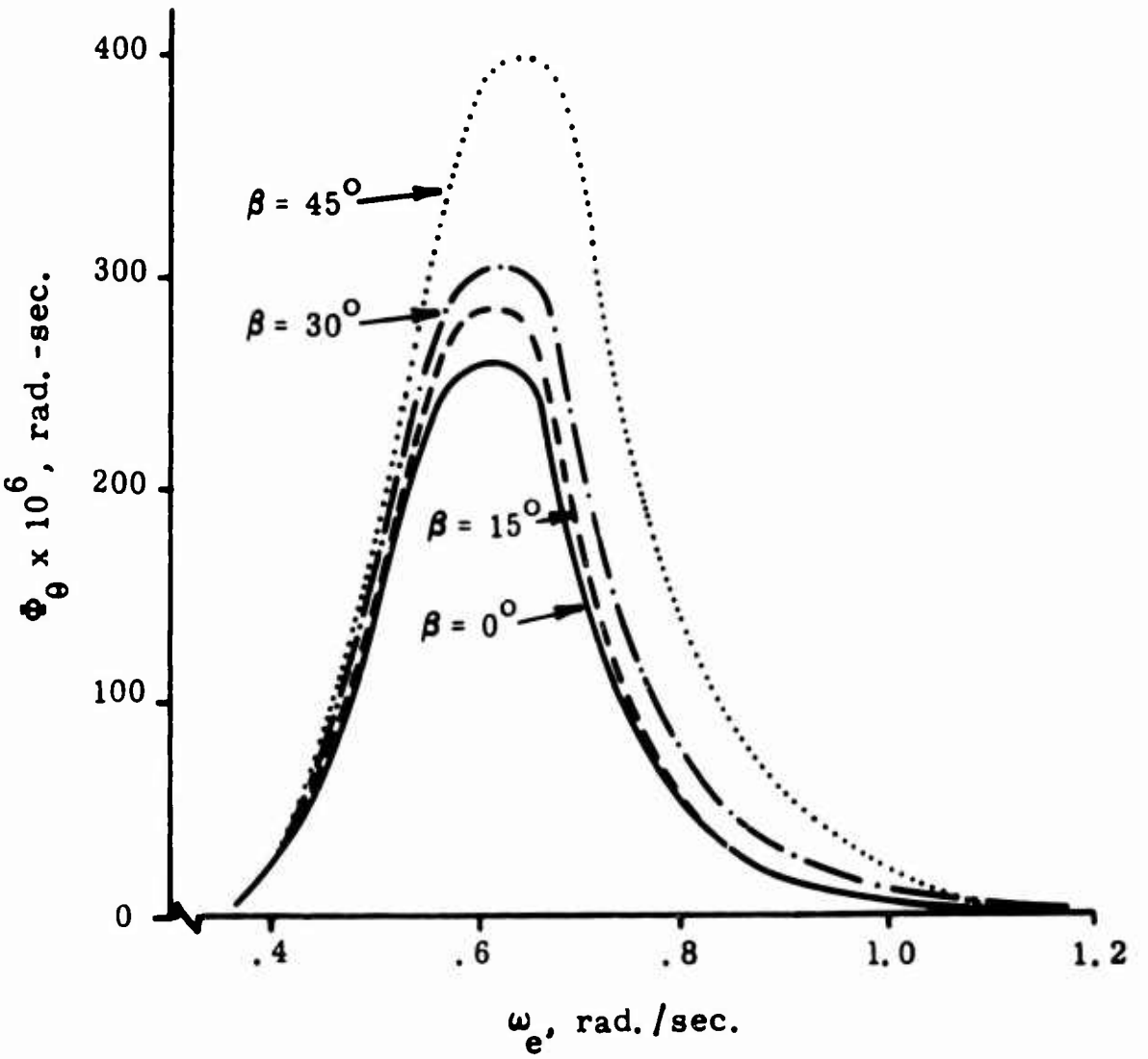

Fig. 22 Pitch spectrum in unidirectional Sea State 6, V = 10 knots

V = 20 knots

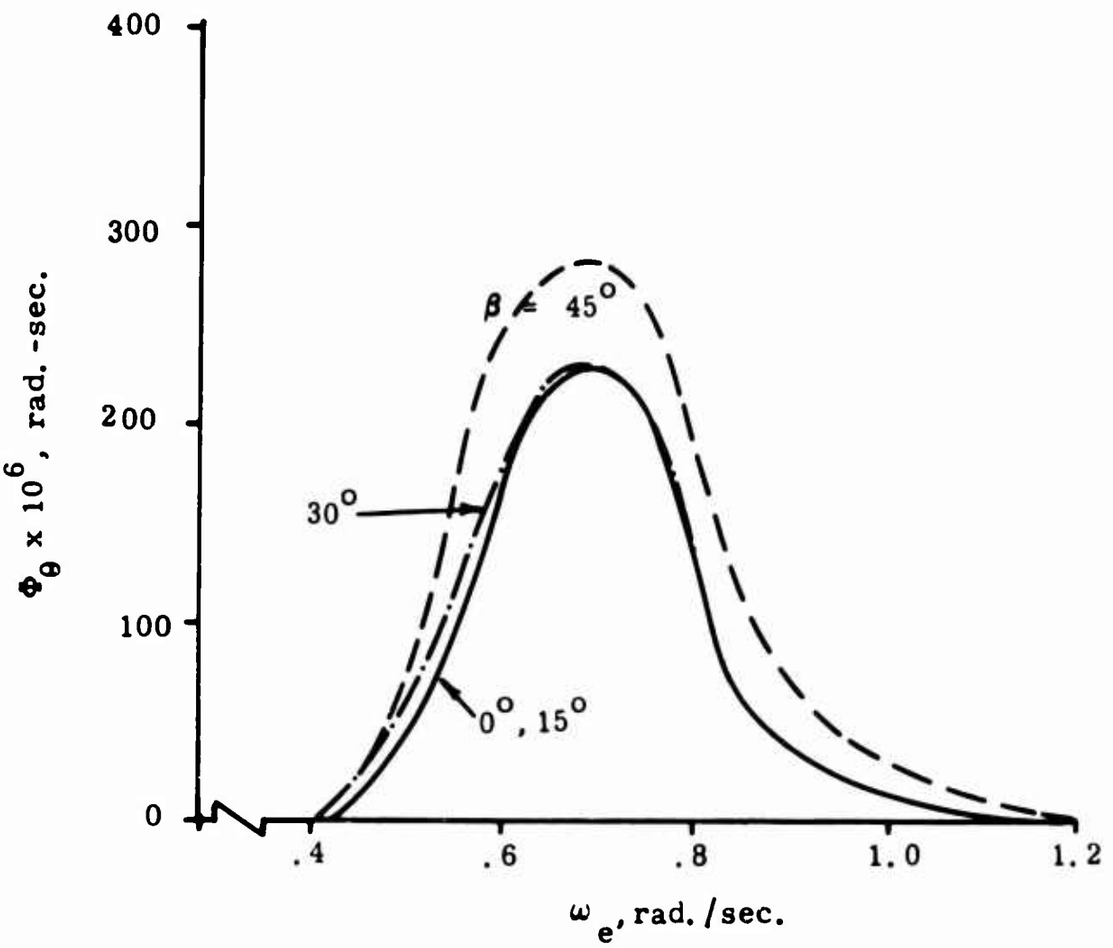

Fig. 23 Pitch spectrum in unidirectional Sea State 6, V = 20 knots

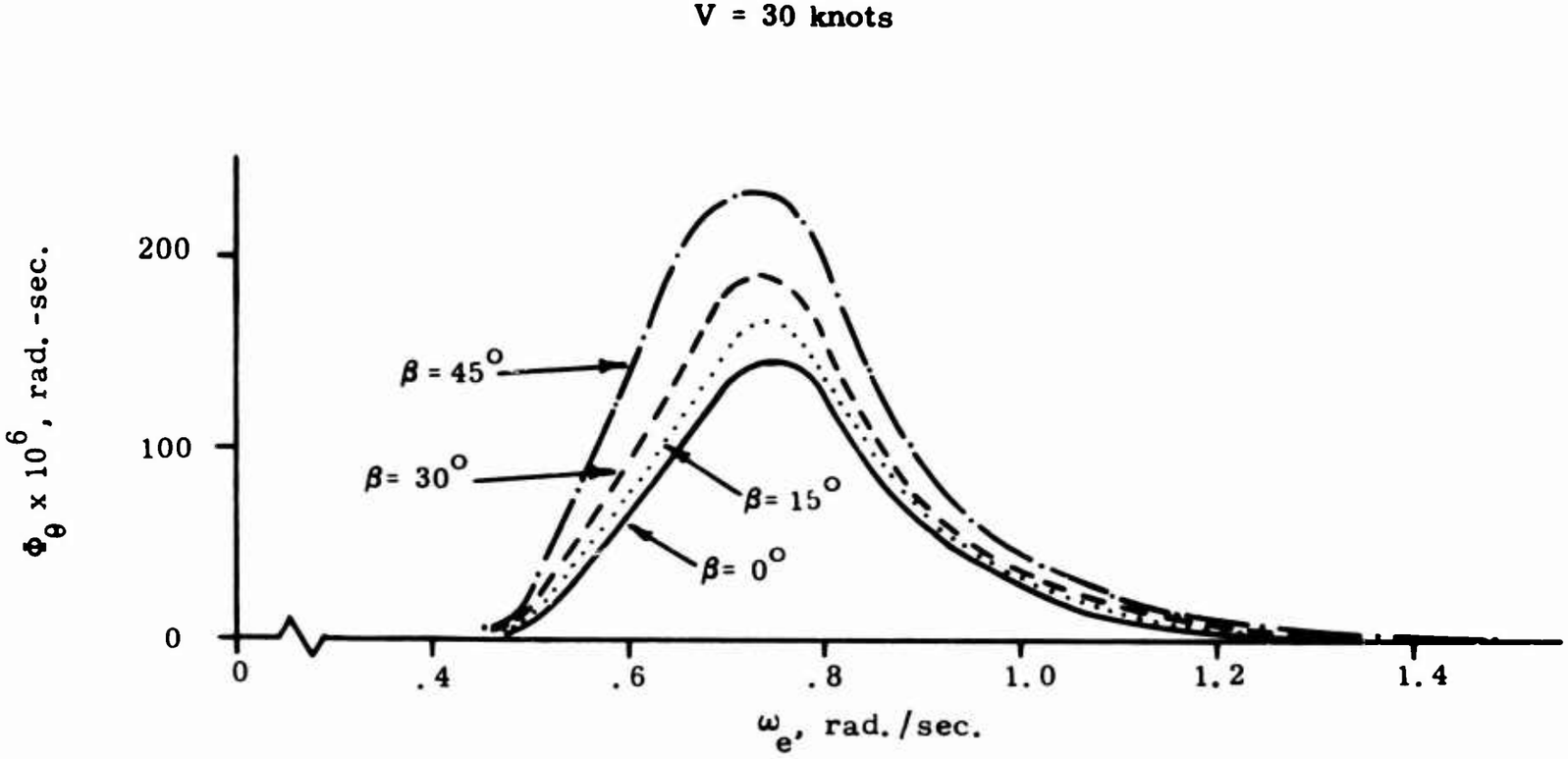

Fig. 24 Pitch spectrum in unidirectional Sea State 6, V = 30 knots

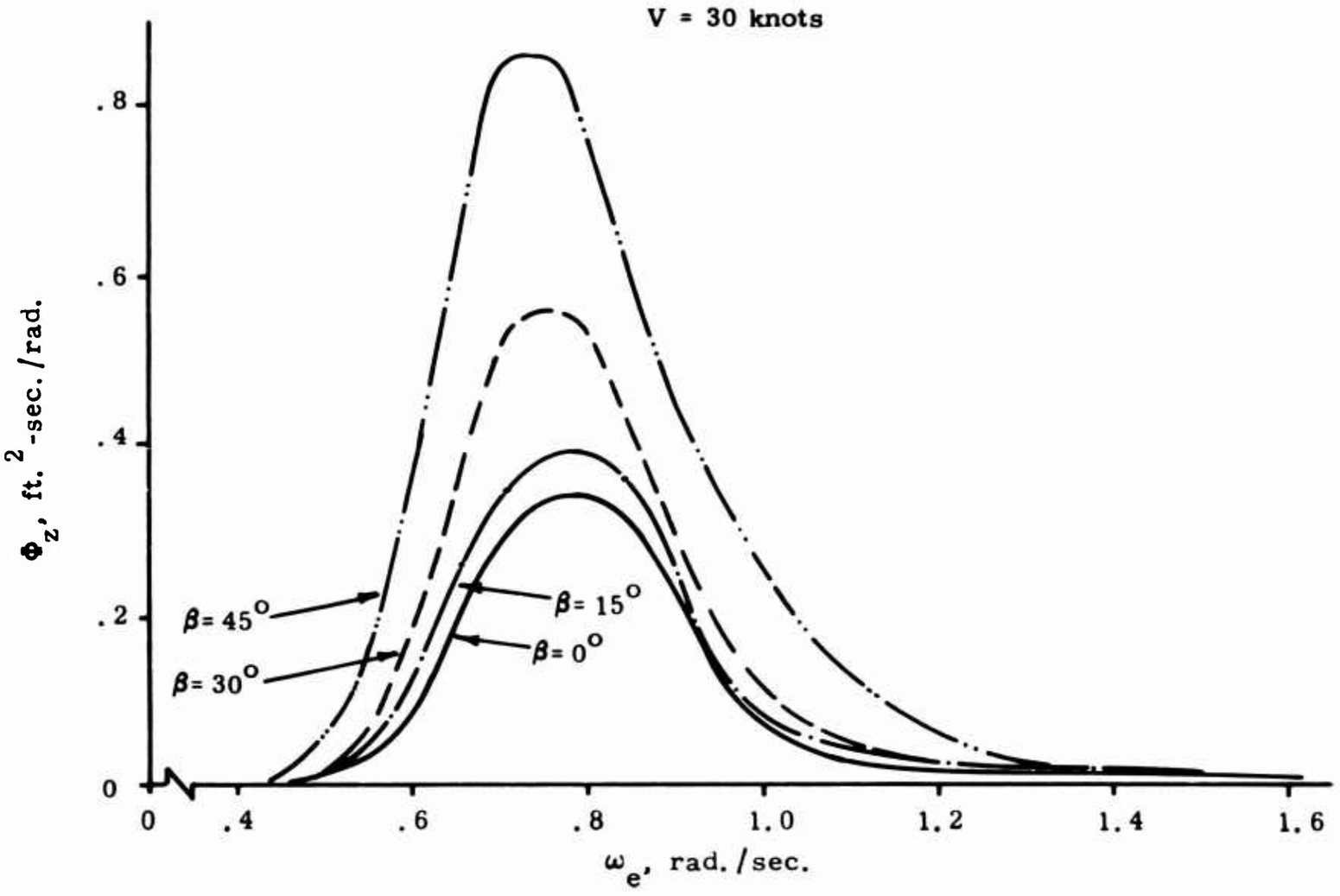

Fig. 26 Heave spectrum in unidirectional Sea State 5, V = 30 knots

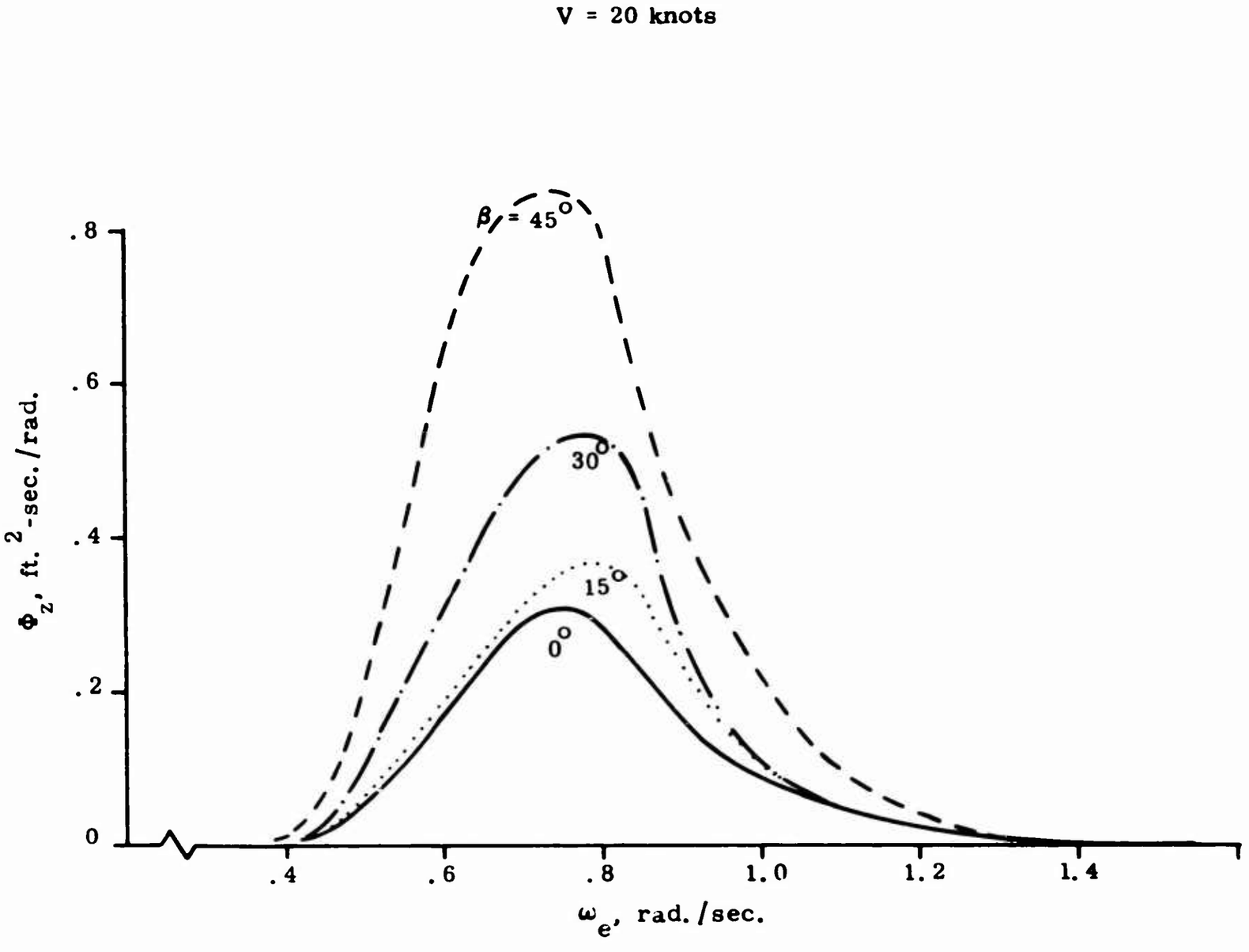

Fig. 25 Heave spectrum in unidirectional Sea State 5, V = 20 knots

V = 20 knots

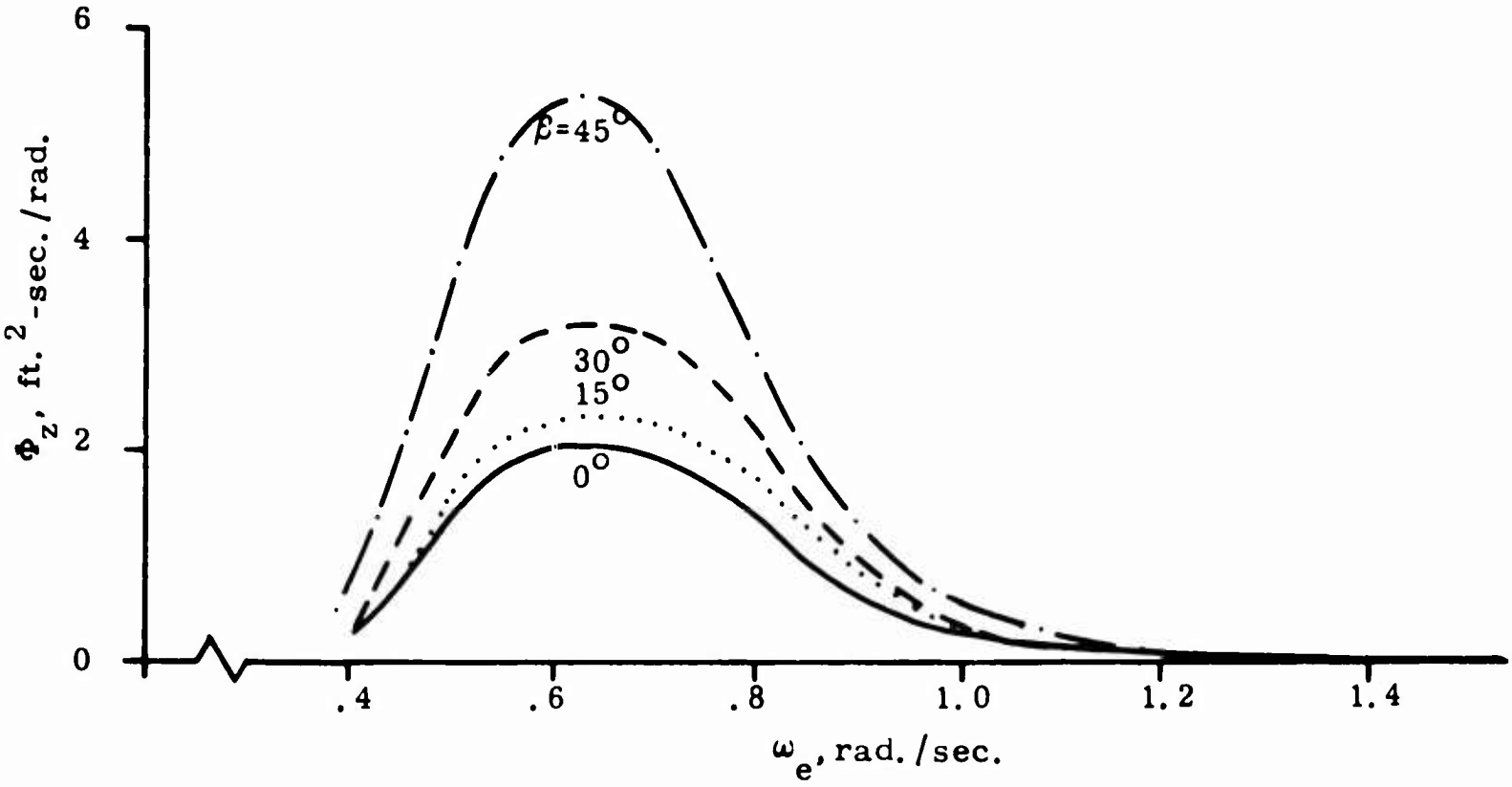

Fig. 27 Heave spectrum in unidirectional Sea State 6, V = 20 knots

V = 30 knots

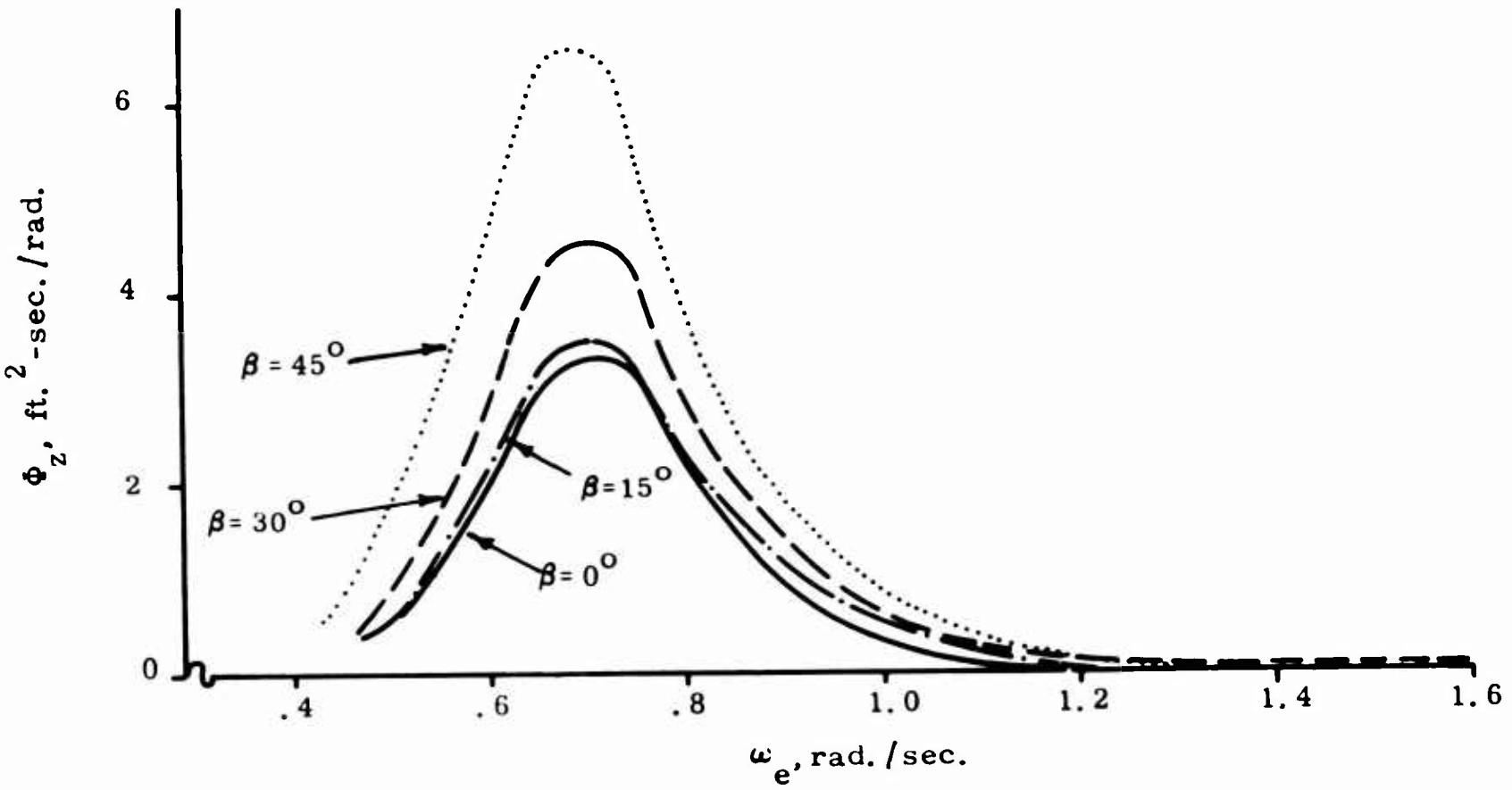

Fig. 28 Heave spectrum in unidirectional Sea State 6, V = 30 knots

V = 20 knots

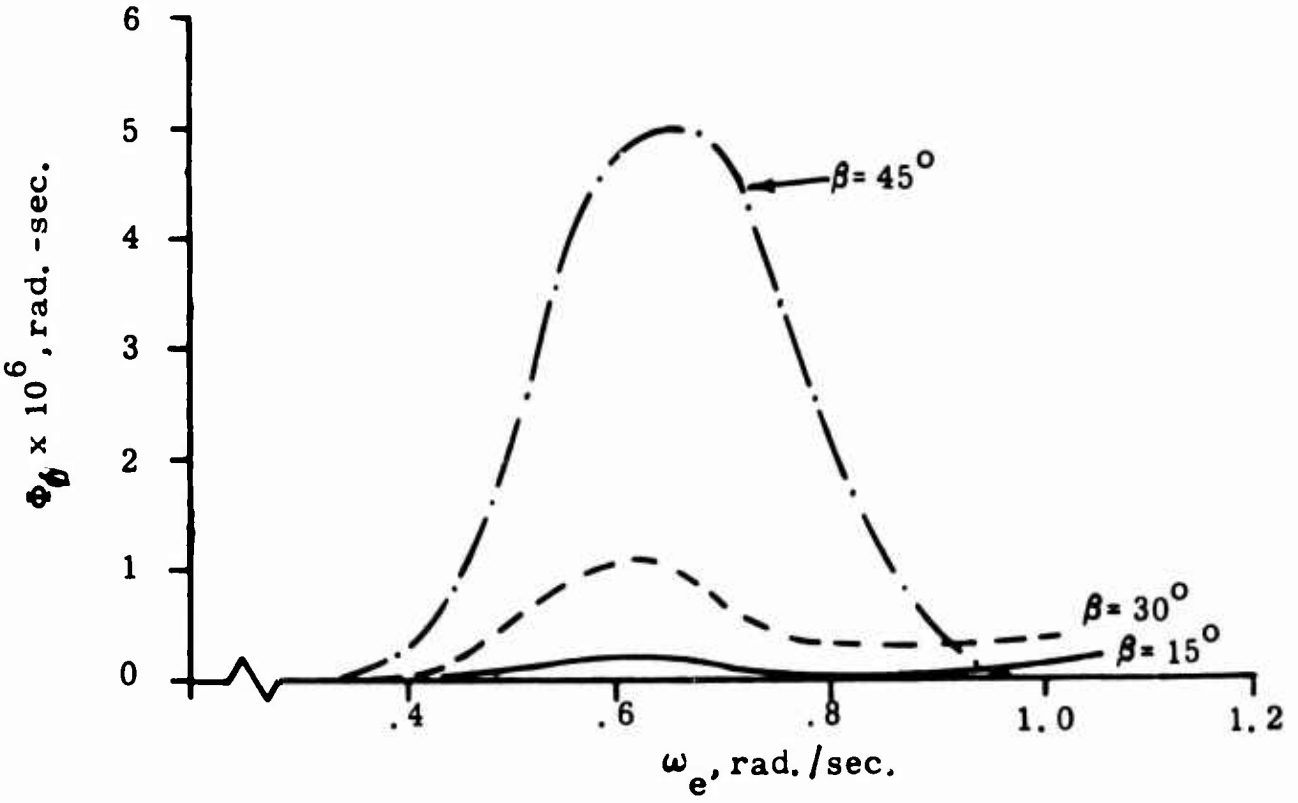

Fig. 29 Roll spectrum in unidirectional Sea State 5, V = 20 knots

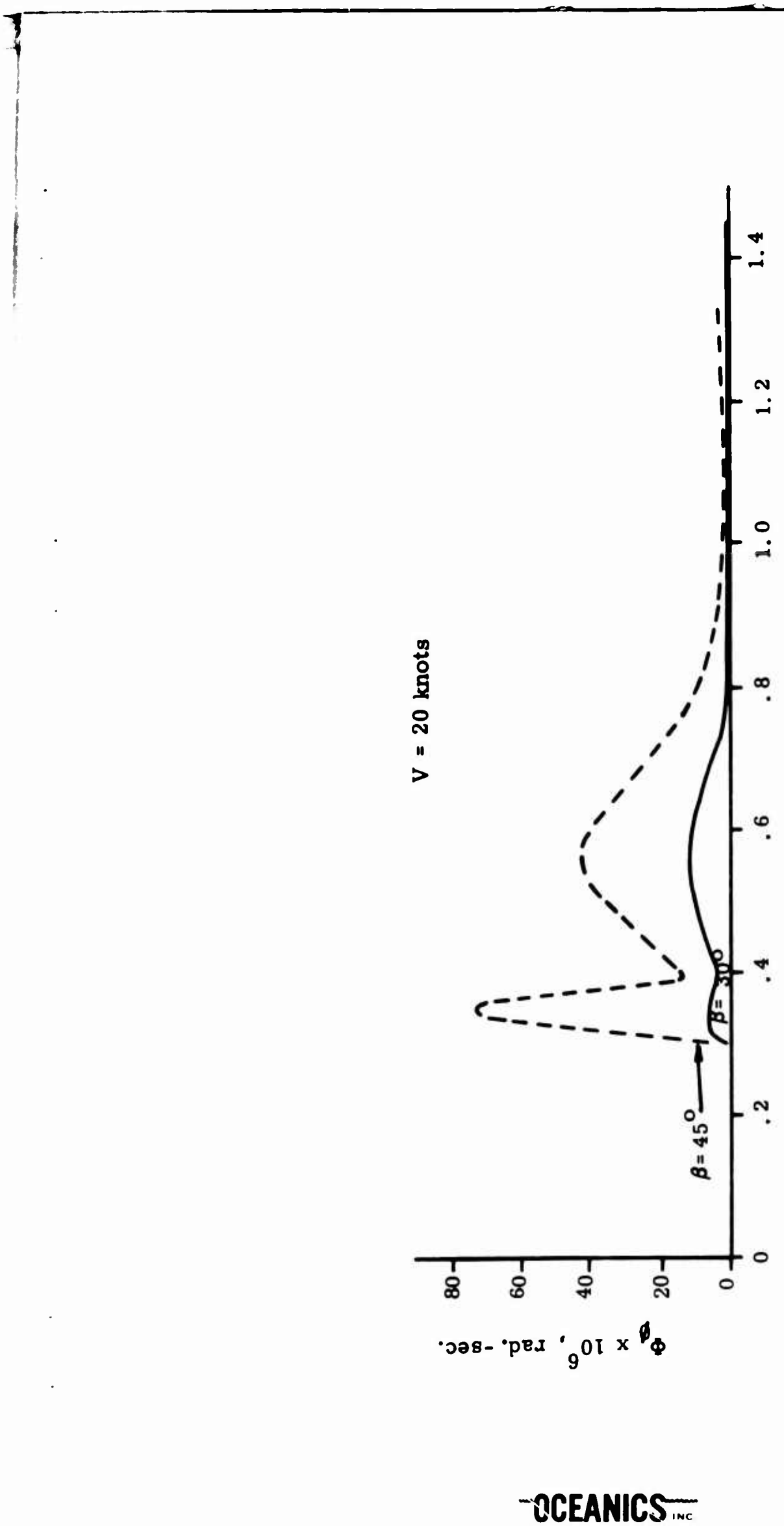

Fig. 30 Roll spectrum in unidirectional Sea State 6, V = 20 knots

V = 10 knots

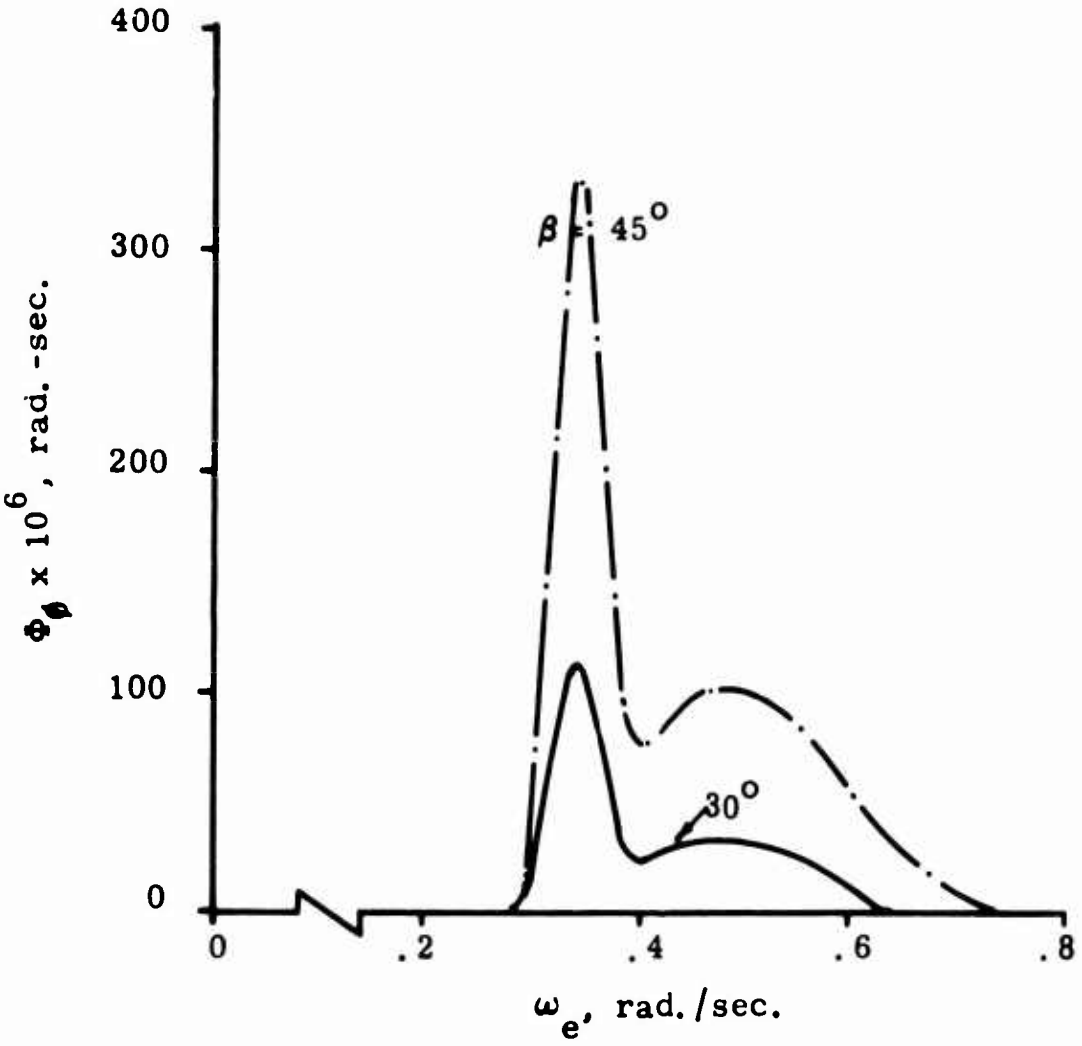

Fig. 31 Roll spectrum in unidirectional Sea State 6, V = 10 knots

UNCLASSIFIED

Security Classification

DOCUMENT CONTROL DATA - R&D

(Security classification of title, body of abstract and indexing annotation must be entered when the overall report is classified)

1 ORIGINATING ACTIVITY *(Corporate author)*

OCEANICS, Inc.
Technical Industrial Park
Plainview, N. Y. 11803

2a REPORT SECURITY CLASSIFICATION

UNCLASSIFIED

2b GROUP

N/A

3 REPORT TITLE

Theoretical Study of the Motions of an Aircraft Carrier at Sea

4 DESCRIPTIVE NOTES *(Type of report and inclusive dates)*

Report on ship motion characteristics, 1 April 1963 to 30 March 1964

5 AUTHOR(S) *(Last name, first name, initial)*

Kaplan, Paul, and Sargent, Theodore P.

6 REPORT DATE	7a TOTAL NO OF PAGES	7b NO OF REFS
January, 1965	84	20

8a CONTRACT OR GRANT NO	9a ORIGINATOR'S REPORT NUMBER(S)
Nonr-4186(00)	65-22
b PROJECT NO	
c RR 011-05-04	9b OTHER REPORT NO(S) *(Any other numbers that may be assigned this report)*
d	None

10 AVAILABILITY/LIMITATION NOTICES

None

11 SUPPLEMENTARY NOTES	12 SPONSORING MILITARY ACTIVITY
None	Director, Air Programs Naval Applications Group Office of Naval Research Washington, D. C. 20360

13 ABSTRACT

A mathematical model is developed for representing the heave, pitch and roll motions of an aircrait carrier at sea. The data is in the form of transfer functions relative to the waves, which are determined for a range of forward speeds and headings considered appropriate to carrier operations during the landing phase. From this information, spectral responses representing the statistical characteristics of motions in certain specific sea states are then developed. The results are presented in a form that can be applied to computer simulation studies for various types of wave disturbances, such as storm conditions, swells, and combinations of such wave systems.

The motions of heave and pitch are emphasized in this study, since roll motions are sufficiently small so that they do not significantly influence the aircraft landing operation. Certain limited conclusions as to motion severity and methods for reducing ship motions are outlined, together with recommendations for specific applications and extensions of the theoretical results.

DD FORM 1 JAN 64 1473

UNCLASSIFIED

Security Classification

14. KEY WORDS	LINK A		LINK B		LINK C	
	ROLE	WT	ROLE	WT	ROLE	WT
AIRCRAFT CARRIERS						
HYDRODYNAMICS						
SHIP MOTIONS						
WAVES						

INSTRUCTIONS

1. ORIGINATING ACTIVITY: Enter the name and address of the contractor, subcontractor, grantee, Department of Defense activity or other organization *(corporate author)* issuing the report.

2a. REPORT SECURITY CLASSIFICATION: Enter the overall security classification of the report. Indicate whether "Restricted Data" is included. Marking is to be in accordance with appropriate security regulations.

2b. GROUP: Automatic downgrading is specified in DoD Directive 5200.10 and Armed Forces Industrial Manual. Enter the group number. Also, when applicable, show that optional markings have been used for Group 3 and Group 4 as authorized.

3. REPORT TITLE: Enter the complete report title in all capital letters. Titles in all cases should be unclassified. If a meaningful title cannot be selected without classification, show title classification in all capitals in parenthesis immediately following the title.

4. DESCRIPTIVE NOTES: If appropriate, enter the type of report, e.g., interim, progress, summary, annual, or final. Give the inclusive dates when a specific reporting period is covered.

5. AUTHOR(S): Enter the name(s) of author(s) as shown on or in the report. Enter last name, first name, middle initial. If military, show rank and branch of service. The name of the principal author is an absolute minimum requirement.

6. REPORT DATE: Enter the date of the report as day, month, year; or month, year. If more than one date appears on the report, use date of publication.

7a. TOTAL NUMBER OF PAGES: The total page count should follow normal pagination procedures, i.e., enter the number of pages containing information.

7b. NUMBER OF REFERENCES: Enter the total number of references cited in the report.

8a. CONTRACT OR GRANT NUMBER: If appropriate, enter the applicable number of the contract or grant under which the report was written.

8b, 8c, & 8d. PROJECT NUMBER: Enter the appropriate military department identification, such as project number, subproject number, system numbers, task number, etc.

9a. ORIGINATOR'S REPORT NUMBER(S): Enter the official report number by which the document will be identified and controlled by the originating activity. This number must be unique to this report.

9b. OTHER REPORT NUMBER(S): If the report has been assigned any other report numbers *(either by the originator or by the sponsor)*, also enter this number(s).

10. AVAILABILITY/LIMITATION NOTICES: Enter any limitations on further dissemination of the report, other than those imposed by security classification, using standard statements such as:

(1) "Qualified requesters may obtain copies of this report from DDC."

(2) "Foreign announcement and dissemination of this report by DDC is not authorized."

(3) "U. S. Government agencies may obtain copies of this report directly from DDC. Other qualified DDC users shall request through _____."

(4) "U. S. military agencies may obtain copies of this report directly from DDC. Other qualified users shall request through _____."

(5) "All distribution of this report is controlled. Qualified DDC users shall request through _____."

If the report has been furnished to the Office of Technical Services, Department of Commerce, for sale to the public, indicate this fact and enter the price, if known.

11. SUPPLEMENTARY NOTES: Use for additional explanatory notes.

12. SPONSORING MILITARY ACTIVITY: Enter the name of the departmental project office or laboratory sponsoring *(paying for)* the research and development. Include address.

13. ABSTRACT: Enter an abstract giving a brief and factual summary of the document indicative of the report, even though it may also appear elsewhere in the body of the technical report. If additional space is required, a continuation sheet shall be attached.

It is highly desirable that the abstract of classified reports be unclassified. Each paragraph of the abstract shall end with an indication of the military security classification of the information in the paragraph, represented as *(TS)*, *(S)*, *(C)*, or *(U)*.

There is no limitation on the length of the abstract. However, the suggested length is from 150 to 225 words.

14. KEY WORDS: Key words are technically meaningful terms or short phrases that characterize a report and may be used as index entries for cataloging the report. Key words must be selected so that no security classification is required. Identifiers, such as equipment model designation, trade name, military project code name, geographic location, may be used as key words but will be followed by an indication of technical context. The assignment of links, roles, and weights is optional.